Evaluating Antibiotic Tolerance Through Osmotic Stress-induced Cross-protection

CHAPTER 1 – INTRODUCTION

Antibiotic resistant microbes are responsible for more than 64.5 million infections and 812,000 deaths worldwide with endemic prevalence in highly populated regions, including the United States [1-4]. Although the United States reports 35,000 deaths from antimicrobial resistance (AMR) each year, estimates, which account for insufficiencies in national reporting rates, suggest as much as 160,000 deaths, placing it as the third leading cause of death [5,6]. AMR has emerged as one of the biggest public health challenges in modern society and is widely accepted as the reason bacteria survive under antibiotic-derived stresses. Effective drug treatment strategies to combat the rise of AMR involve therapeutic interventions which consider the biology of the pathogen(s) along with the environmental context of infection.

Upon infection in mammalian hosts, many pathogens experience modifications in environmental temperature, which are sensed through sensory mechanisms which trigger transcriptional changes for adaptation. For pathogens that must translocate to a more favorable physiological niche for infection, heat-shock proteins are induced transiently in response to temperature stress to cope with protein damage and to maintain membrane homeostasis [7]. Conversely, if the host environment is sufficient for infection onset, expression of thermoregulated virulence genes are activated, which activate host inflammatory responses, subjecting the pathogens to oxidative and nitrosative stress [8,9]. Cell stress responses activate interconnected regulatory networks, which allow pathogens to adapt and sense different colonization niches. In fact, there is considerable overlap in genes activated through these networks which are not exclusive to environmentally induced stresses, but also include antibiotic, and, as a byproduct, antibiotic-induced oxidative stresses [10].

Bacterial cells respond to antibiotic stress in a multitude of ways, with mechanisms behind resistance being the most well studied, in addition to more recent observations of tolerance and persistence [11]. Common mechanisms of antibiotic resistance involve genetic mutations that allow the cells to inactivate the drugs, modify drug targets, decrease uptake, or increase efflux [12,13]. Resistant cells grow at elevated antibiotic concentrations, and are most commonly detected with MIC (minimum inhibitory concentration) measurements, the lowest concentration that will inhibit or kill actively growing cells [14]. However, resistance is not the only way bacteria can withstand the stress of antibiotics. Another way bacteria survive under the bactericidal action of antibiotics is known as tolerance, where cells are still genetically susceptible, yet phenotypically tolerant to treatment [15]. Tolerant cells play a pivotal role in causing recurrent and chronic infections due to their ability to survive antimicrobial treatment, and, depending on the degree of antibiotic stress encountered, develop adaptive responses that allow them to survive under stress [16]. Tolerant populations of cells exhibit minimal to no difference in the MIC, but can survive antibiotic stress at concentrations much higher than the MIC [17,18]. Thus, tolerant cells are quantified by measuring the minimum duration of killing (MDK) and/or the minimum bactericidal concentration (MBC) of the population. MDK is the time it takes for an antibiotic to reduce the size of the population by a certain percentage (e.g., 99%), while MBC is the concentration required to kill ≥99.9% of the bacterial population [18,19]. A tolerant sub-population of bacteria that resist antimicrobial action are termed “persisters", and similarly to whole-population tolerant cells, are not heritable [17,21-23]. Thus,

regrowth of a subpopulation of persister cells to a largely non-tolerant population occurs when stress conditions dissipate [20].

The adaptive responses of antibiotic stress, observed through alterations in phenotypical and physiological characteristics, are shared between whole-population level tolerant and sub-population level persister cells [24,33]. Evolution studies in response to antibiotic stress have revealed shared responses between resistant and tolerant cells. *Escherichia coli* (*E. coli*) populations resistant to streptomycin, ciprofloxacin, and carbenicillin evolved over 11 days yield mutations in core metabolic genes, notably 2-oxoglutarate dehydrogenase (*sucA*), which is also implicated in tolerance along with its mutually essential, multienzyme complex counterpart *sucB* [25-29]. Expression of *sucA* is also implicated in cells subject to oxygen, nutrient, and osmotic stress through both transient alterations in gene expression and genetic mutations, suggesting the overlapping role of this gene in conferring tolerance to antibiotic and environmental stresses [30,31]. In addition, *tolC*, a gene encoding for an outer membrane efflux protein, has been implicated in both antibiotic resistance and tolerance as well as in response to nutrient and osmotic stress, suggesting that adaptations to stresses are not specific to metabolic enzymes, but exist through interconnected regulatory networks involving shared mechanisms [32-35]. Since antibiotic tolerance has been shown to facilitate the evolution of resistance, strategies to prevent tolerance, or eradicate tolerant cells through repotentiation to antibiotics, will need to account for associated genetic adaptations perpetrated by environmental stresses [56-59].

The general and specific stress responses help cells survive the conditions of the current stress, as well as subsequent higher levels of the same stress [63,64]. This phenomenon is termed "cross-protection", which not only explains protection against increased levels of the same stress, but also against different stresses [65-69]. The fitness benefit carried to additional stresses is non-specific and leads to antibiotic tolerance and resistance [70-73]. In fact, cells exposed to bacteriostatic antibiotics exhibit increased fitness to subsequent antibiotic treatment, and cells exposed to both bacteriostatic and bactericidal antibiotics confer adaptations to acidic stress [74,75]. As research into cross-protection has provided insight into pre-adaptations to successive stresses, studies have lacked investigation into co-adaptations through simultaneous exposure to stresses, conditions that are far more likely to be encountered by cells in physiological environments.

Bacteria encounter osmotic stress, in particular, throughout diverse physiological niches in the human body, especially at sites which pose a greater risk of recalcitrant infections [36, 37]. Cells must cope with large fluctuations in extracellular osmotic environments that occur over a range of timescales. Enteric bacteria, such as *E. coli*, traverse between sites of dynamic osmolarity fluctuations, such as the blood, intestines, and urinary tract [37,40,41]. In fact, *E. coli* urinary tract infections develop due to the translocation of enteric strains to the urinary tract [37]. Bacteria in antibiotic-tolerant biofilms, a common state of bacterial infection in wounds and intravenous and urinary catheters experience transitions of high and low osmolarity, and, consequently, sustain associated responses between both stresses [36-39]. Additionally, adaptive mutations that confer increased fitness in response to one osmolyte can extend to other osmolytes [31].

Bacterial cell response to osmotic stress has been well documented [42]. In addition to maintaining a high level of cytosolic osmotic pressure, a rigid cell envelope is necessary for cells to sustain the osmotic pressures of the environment and to prevent lysis [43]. Compatible solutes, such as proline, glycine betaine, and glutamate, are utilized by cells to regulate internal osmolarity [44-46]. The stress response also influences growth rate by decreasing the rate of

translation-dependent ribosomal elongation and by altering metabolic processes through limitation of glucose uptake and the shuttling of carbon sources from the TCA cycle for metabolic downregulation and osmoprotectant biosynthesis [47-49]. The overall impact on instantaneous growth rate, however, is not affected by hyperosmotic conditions, indicating that cells quickly buffer against osmotic changes to resume normal growth [50]. Alterations in fatty acid saturation and phospholipid composition lead to changes in membrane composition [10]. Specifically, the upregulation of cardiolipin biosynthesis, an anionic phospholipid, leads to increases in the proportion of anionic phospholipids to zwitterionic phospholipids in the membrane [51]. Increases in cardiolipin is observed when energy metabolism is impaired with antibiotics [52,53]. These responses are not specific to osmotic stress, as antibiotic tolerant cells display perturbations in membrane integrity, observed by decreases in membrane potential (MP), and changes in metabolism, such as lowered basal respiration, downregulated TCA cycle, and dissipation of the proton motive force (PMF) (**Fig. 1.1**) [26,29,54,55].

At present, very little is known about the development of tolerance in response to osmotic stress. Although cells undergo similar adaptations to both antibiotic and osmotic stress, there exists a need to elucidate the relationship, observed through growth rate patterns, metabolic perturbations, and membrane alterations, in response to simultaneous exposure to both stresses. A better understanding of these interactions will produce new strategies for treating persistent and recalcitrant bacterial infections.

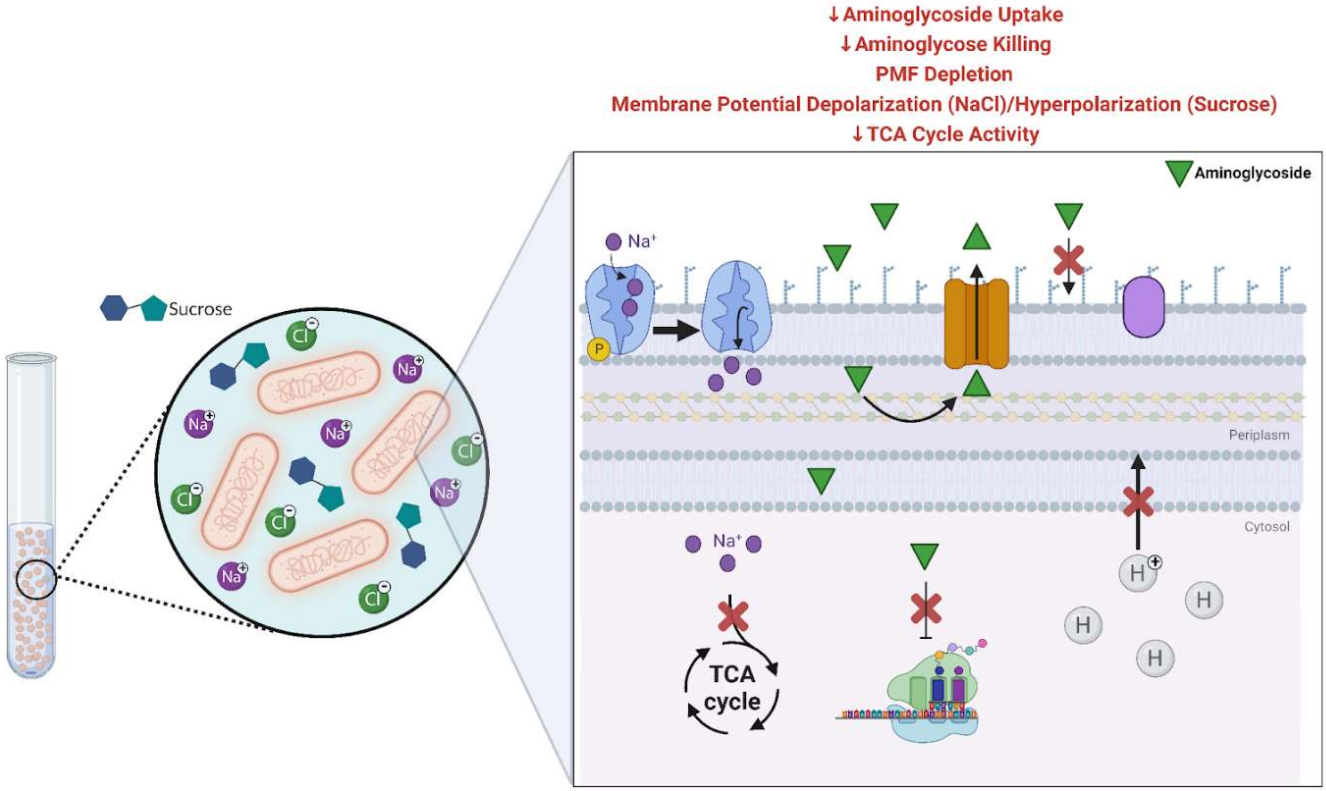

Figure 1.1 - Schematic representation of osmotic stress-induced antibiotic tolerance. *E. coli* MG1655 exposure to NaCl and sucrose induces antibiotic tolerance to aminoglycoside antibiotics. Tolerance responses include decreased antibiotic uptake and killing, depletion of the PMF, membrane depolarization (NaCl) or hyperpolarization (sucrose), and decreased TCA cycle activity.

CHAPTER 2 – DEMONSTRATING OSMOTIC STRESS-INDUCED CROSS-PROTECTION THROUGH TIME-KILL KINETICS

2.1 Introduction

The adaptive responses to stress occur at the transcriptional, translational, and post-translational levels, as bacteria are able to regulate their response through changes in gene expression, protein activity, and metabolism [60,61]. Even as responses to environmental stresses vary due to the types of stress and the metabolic state, cells regularly, and successively, respond to stresses through fluctuations in growth patterns. Specifically, stressed cells experience deleterious consequences on growth, accompanied by low metabolic states which give rise to mutations that allow cells to survive the duration of stress [61]. Bacterial stress responses not only encourage adaptation, but also promote pathogenicity in stressful environments, conferring protective effects through slow growth which enable synergistic protective responses between stresses [62].

Adaptive responses in metabolic genes may be shared between cells that are osmotically stressed and resistance to antibiotics. For example, *sucA* is a TCA cycle metabolic gene mutated in cells resistant to antibiotics, but the gene is also implicated in cells subjected to osmotic stress. Genes implicated in antibiotic efflux, such as *tolC*, are also observed in responses to NaCl, resistance, and tolerance to antibiotics [25-35,84]. Although adaptive responses overlap between both osmotic and antibiotic stresses and may contribute to cross-protection, the fitness advantage conferred from the response of osmotic stress in antibiotic tolerance is not well understood. Evidence of osmotic stress-induced cross-protection of antibiotics has been demonstrated in a resistance model, showing up to 4-fold increases in MIC when *E. coli*, *Salmonella enterica* serovar Typhimurium, and *Staphylococcus aureus* were co-exposed to high NaCl concentrations and bactericidal/static antibiotics [76]. In a bacteriostatic tolerance model, high NaCl concentrations rescued the growth rate of *E. coli* during treatment with chloramphenicol and tetracycline [35]. Although transitions in growth rate is indicative of antibiotic tolerance, established models best explain tolerance by utilizing bactericidal, instead of bacteriostatic, antibiotics [77,78]. The reasons for this are derived from clinical relevance, as bactericidal treatments show the greatest clinical efficacy for recurrent UTI and catheter-associated infections [36,79,80]. These types of infections are perpetrated by bacterial biofilms which provide a favorable niche for the generation of slowly growing, energy depleted tolerant cells [36,77,78].

Osmotic stress is a dominant stress source in biofilms, and is responsible for up-regulation of sporulation, extracellular polymeric substances (EPS), and capsulation [81-83]. If unchecked, the presence of osmotic stress, paired with the slow growing tolerant population, allows for the evolution to resistance [56-59]. Therefore, growth assays, such as MIC and time-kill analysis, will provide detailed insight into cross-protective effects of osmotic stress in response to clinically-relevant bactericidal antibiotics. However, time-kill assays provide an advantage over MIC by establishing the rate of killing over a range of concentrations, allowing for dynamic time measurements of antibiotic efficacy. In this context, we hypothesize that antibiotic tolerance is induced through simultaneous exposure to osmolytes (NaCl and sucrose) and bactericidal antibiotics. Additionally, we propose that time-kill kinetics will best demonstrate the growth rescue phenotype in cross-protected and tolerant *E. coli* populations.

2.2 Materials and Methods

2.2.1 Bacterial Strains and Growth Conditions

The bacterial strain used in this study was *E. coli* K-12 substr. MG1655. Freezer stocks were streaked onto Lysogeny broth (LB) agar (IBI Scientific) plates and grown overnight (O.N.). O.N. shaking cultures were inoculated from a single colony from the streaked plate into 3 mL of M9 (1 x M9 minimal medium with 0.4% glucose, 2mM $MgSO_4$, and 0.1mM $CaCl_2$) (Sigma-Aldrich) and grown overnight at 37˚C on an orbital shaker at 250 rpm. The overnight culture was diluted 1:225 into M9 and cultures were grown for 4 h (subculture). After subculture, cells were washed 3x by centrifugation at 5,000 x g for 5 minutes in M9 and the final suspension was resuspended in M9. The final cell density was adjusted to 0.05 OD and cells were grown in M9 for 4 h (early to mid-exponential phase) with/without presence of NaCl (Macron Fine Chemicals), sucrose (Fisher Scientific), and antibiotics. The antibiotics used were kanamycin, tobramycin, ampicillin, and norfloxacin (all purchased from Fisher Scientific), at concentrations determined through time-kill assays as several times greater than the MIC (i.e., the highest concentration that allows colony growth within the countable range after cells have been exposed to each antibiotic for 4 h).

2.2.2 Time-kill Assay for Tolerance Measurements

Survival assays were performed to measure tolerance in stressed cells. Colony Forming Units (CFU) were measured at the beginning and end of 4 h exposure to each antibiotic used in this study. For each time point, an aliquot of each sample was added to the wells of a flat bottom 96-well microplate with ten-fold serial dilutions in sterile PBS were carried out in duplicates. Spread plates were made with 50 µL of each dilution added onto an LB-agar plate along with 5-10 beads and shaken for 15-30 seconds. Plates were incubated in 37°C overnight and colonies were counted. CFU/mL values were calculated by dividing the number of the colonies by 50 µL and multiplying the results by dilution factor (e.g. 10^5) and 1000 as a unit conversion from µL to mL. This results in the CFU/mL value for each condition and the percent survival was calculated by 100 x (the CFU/mL of remaining viable cells (at 4 hr))/(the CFU/mL of the initial culture (at 0 hr)). Finally, the percent survival was log transformed and plotted on a bar graph. Two biological replicates and two technical replicates per condition and dilution factor were used for the tolerance measurements.

2.3 Results

To quantify the magnitude of cross-protection, our previous work measured the MIC_{50} of cells co-exposed to osmolytes and gentamicin, a bactericidal aminoglycoside (Ranjbar, 2020, Chapter 5) [84]. The two osmolytes chosen represent two different classes, ionic (NaCl) and non-ionic (sucrose). Sucrose was chosen because *E. coli* K-12 substr. MG1655 does not preferentially metabolize it as a carbon source [85]. However, slow growing and enteropathogenic *E. coli* can metabolize sucrose, indicating its usefulness to study as an osmolyte in tolerance formation [86]. The osmolarity of the 0.5M NaCl and 15% sucrose solutions (dissolved in M9) were 1.3 and 0.7 Osm/L, respectively. We found that a 20 h exposure to osmolytes did not significantly impact *E. coli* resistance to gentamicin [84]. The MIC_{50} values (inhibiting grown in 50% of population) for all three conditions (NaCl + gentamicin, sucrose + gentamicin, gentamicin only) were

approximately 3 mg/mL, suggesting that the osmolytes had an insignificant effect on gentamicin resistance.

Time-kill assays have been shown to identify antibiotic tolerance by measuring survival of bacteria at different time points during exposure to the antibiotic [18,87]. We performed survival assays at 0 h (lag phase) and 4 h (early to mid-exponential phase) to demonstrate the cross-protective effects of osmotic stress in response to antibiotic stress. Antibiotics from three different classes: aminoglycosides, β-lactams, and fluoroquinolones were chosen due to their frequent use in clinical treatment of recurrent infections [80,88,89]. Concentrations of antibiotics used were determined through time-kill assays, as cells were challenged to a range of concentrations over a 4 hr period. We selected the highest concentration of each antibiotic after 4 hrs of killing, which, after spread plating without dilution, exhibited countable growth (400-4000 CFU/mL). We designated the concentration for each antibiotic as the lethal concentration limit (LCL). Subjecting cells to the LCL, followed by growth rescue using osmolytes, effectively incorporates the $MDK_{99.9}$ tolerance assay parameter by delaying the duration of killing of 99.9% of the population relative to osmolyte-free conditions.

2.3.1 The cross-protective effects of osmolytes against aminoglycosides

We first tested the aminoglycosides kanamycin (Kan) and tobramycin (Tob) for cross-protection using a range of concentrations of NaCl (up to 0.5M) and sucrose (up to 25%). The LCL of Kan and Tob were determined to be 5.5 μg/mL and 0.75 μg/mL, respectively (see 2.2.2 and 2.3). After 4 h of exposure to Tob, only 0.0034% of cells survived (**Fig. 2.2**), whereas 0.071% of cells survived Kan treatment (**Fig. 2.1**). When cells were co-exposed to each antibiotic and 0.25M NaCl, survival increased to 360% and 680% against Kan and Tob, respectively (**Figs. 2.1 and 2.2**). The growth rescue effect of 0.25M NaCl, which was greater than 0.5M NaCl, represented 5,100x and 200,000x factor increases in *E. coli* tolerance to Kan and Tob, respectively. The survival of cells exposed only to 0.25M (690%) and 0.5M NaCl (51%) had similar growth outcomes when compared to cells that were cross-protected; however, there was a stronger association in survival between cells cross-protected to Tob by NaCl and exposure to NaCl only, with differences of only 10% in survival with 0.25M NaCl and no difference in survival with 0.5M NaCl (**Fig. 2.2**). It is worth noting that even though Tob exhibited a larger killing effect compared to Kan (0.0034% vs 0.071% survival), the degree of cross-protection by NaCl was greater in Tob-treated cells.

Increases in aminoglycoside survival extended to cells cross-protected by sucrose. The degree of cross-protection was the greatest in 25% sucrose, with increased survival against both Kan (38%) and Tob (19%) (**Figs. 2.1 and 2.2**). Sucrose addition improved the tolerance of cells exposed to Kan and Tob, resulting in 540x and 5,600x factor increases in growth, respectively. Exposure to a lower concentration of sucrose (15%) resulted in 2.4x and 120x factor increases in tolerance to Kan and Tob, respectively. Similarly to NaCl, sucrose addition was not lethal to cells, with a 190% increase in survival to 15% sucrose, and a 170% increase to 25% sucrose (**Figs. 2.1 and 2.2**). However, cells did not show similar patterns in cross-protection between NaCl and sucrose; growth was recovered to equivalent osmolyte-only levels with NaCl, whereas growth in sucrose-only cells was higher relative to cross-protected cells.

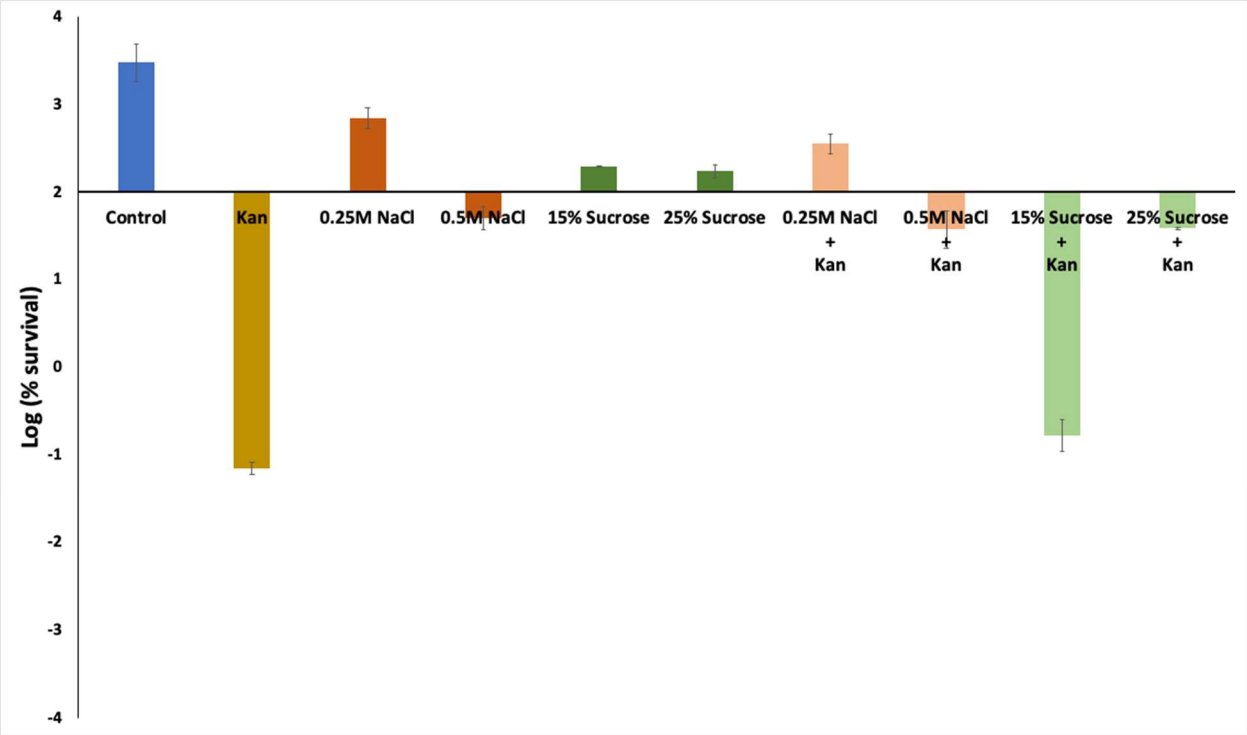

Figure 2.1 - Exposure to osmolytes increases *E. coli* survival to 5.5 µg/mL kanamycin. The plot shows log percent survival of cells in Control (± Kan), 0.25M & 0.5M NaCl (± Kan), and 15% and 25% Sucrose (± Kan). All log percent survival values are averages of viable CFUs after 4 h exposure with/without 5.5 µg/mL kanamycin in 2 biological replicates and 2 technical replicates for each biological replicate in each condition. Error bars represent standard deviations.

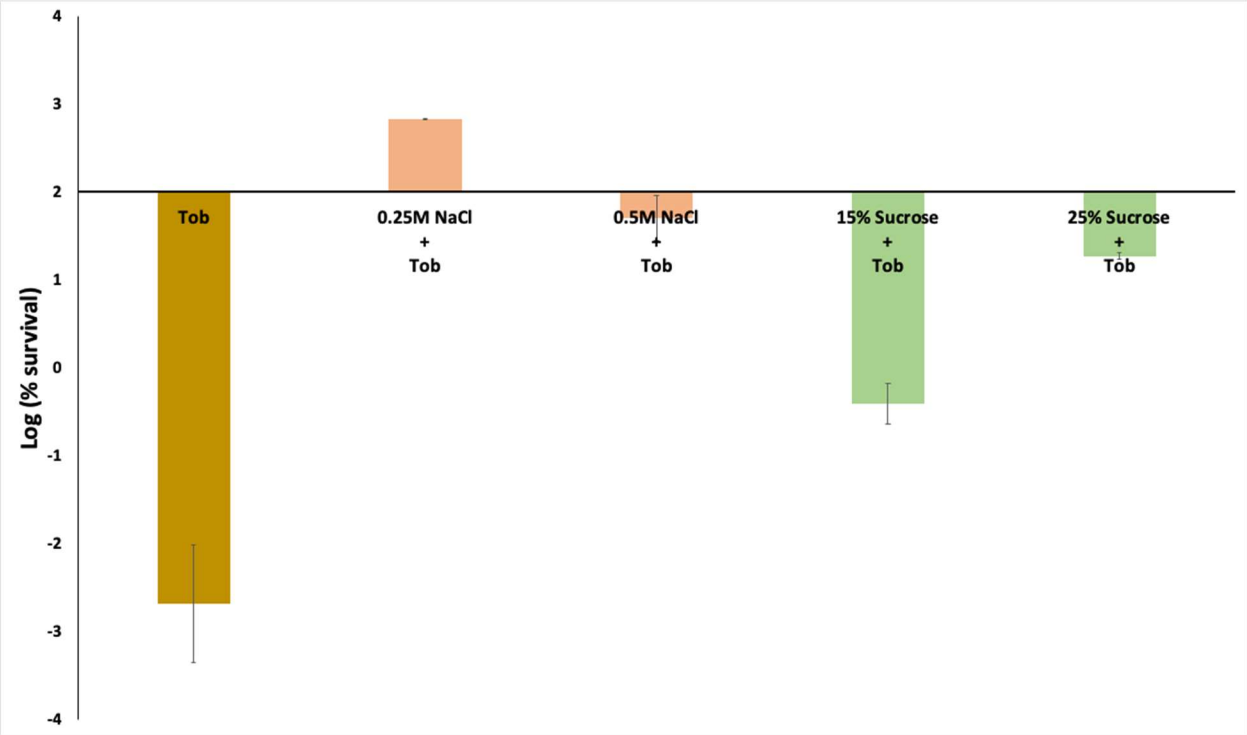

Figure 2.2 - Exposure to osmolytes increases *E. coli* survival to 0.75 µg/mL tobramycin. The plot shows log percent survival of cells in Control (+ Tob), 0.25M & 0.5M NaCl (+ Tob), and 15% and 25% Sucrose (+ Tob). Control values for each condition are omitted as they are displayed in Fig 2.1. All log percent survival values are averages of viable CFUs after 4 h exposure with 5.5 µg/mL tobramycin in 2 biological replicates and 2 technical replicates for each biological replicate in each condition. Error bars represent standard deviations.

2.3.2 The cross-protective effects of osmolytes against β-lactam and fluoroquinolone antibiotics

To determine if cross-protection was specific to aminoglycosides or shared across different classes of bactericidal antibiotics, we performed survival assays against ampicillin (Amp), a β-lactam, and norfloxacin (Nor), a fluoroquinolone. The LCL of Amp and Nor were determined to be 40 µg/mL and 1 µg/mL, respectively (see 2.2.2 and 2.3). After 4 h of exposure to Amp, only 0.0053% of cells survived (**Fig 2.3**), whereas 0.072% of cells survived Nor treatment (**Fig 2.4)**. Relative to aminoglycosides, the same levels of osmolyte exposure (up to 0.5M NaCl and 25% sucrose) in cells treated with Amp and Nor did not confer similar magnitudes of growth rescue (**Figs. 2.3 and 2.4**) Therefore, the osmolyte concentration range was increased to 1M NaCl and 35% sucrose. When cells were co-exposed to each antibiotic and 1M NaCl, survival increased to 38% and 120% against Amp and Nor, respectively (**Figs. 2.3 and 2.4**). The growth rescue effect represented 7,200x and 1,700x factor increases in tolerance to Amp and Nor, respectively (**Figs. 2.3 and 2.4**). Compared with aminoglycosides, which showed up to a 200,000x factor increase in protection with NaCl, these increases in growth are comparatively less pronounced. Similarly to aminoglycosides, however, cells that were cross-protected by NaCl exhibited similar growth outcomes compared to cells exposed only to the osmolyte. This was observed only at a much higher concentration (1M NaCl), with a difference of 15% with Amp and a 57% gain in growth with Nor. When compared to aminoglycosides, these results suggest that a much higher concentration of NaCl is needed in non-aminoglycoside antibiotics to confer a similar survival advantage.

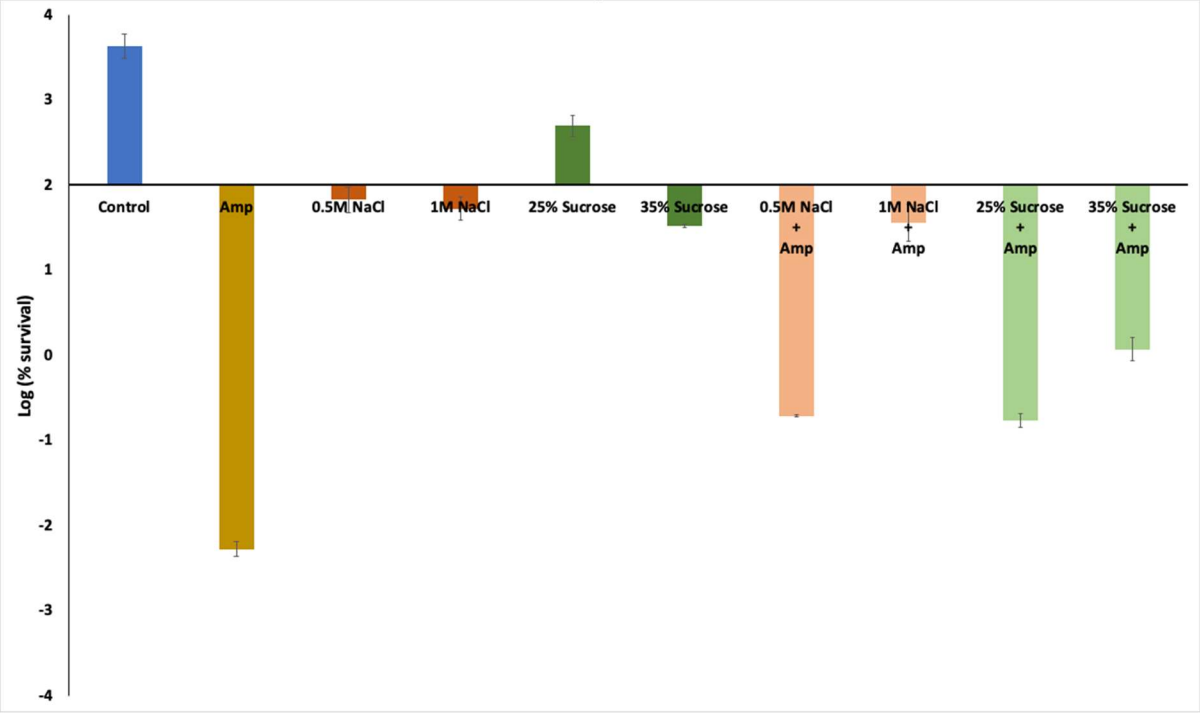

Figure 2.3 - Exposure to osmolytes increases *E. coli* survival to 40 µg/mL ampicillin. The plot shows log percent survival of cells in Control (± Amp), 0.5M and 1M NaCl (± Amp), and 25% and 35% Sucrose (± Amp). All log percent survival values are averages of viable CFUs after 4 h exposure with/without 40 µg/mL ampicillin in 2 biological replicates and 2 technical replicates for each biological replicate in each condition. Error bars represent standard deviations.

Increases in β-lactam and fluoroquinolone survival extended to cells cross-protected by sucrose. Similarly to NaCl, the degree of cross-protection was the greatest with the highest concentration of sucrose (35%) across both antibiotic classes; however, survival was still lower overall relative to 1M NaCl. Survival against Amp and Nor increased to 1.2% and 9.7%, respectively, when co-exposed to 35% sucrose (**Figs. 2.3 and 2.4**). Sucrose addition improved the tolerance of cells exposed to Amp and Nor, resulting in 230x and 140x factor increases in growth, respectively. Although high levels of osmolytes (1M NaCl & 35% sucrose) slowed growth of cells, osmolyte treatment alone was not lethal (**Figs. 2.3 and 2.4**). Additionally, growth was recovered to equivalent osmolyte-only levels with cells cross-protected by 1M NaCl and 35% sucrose.

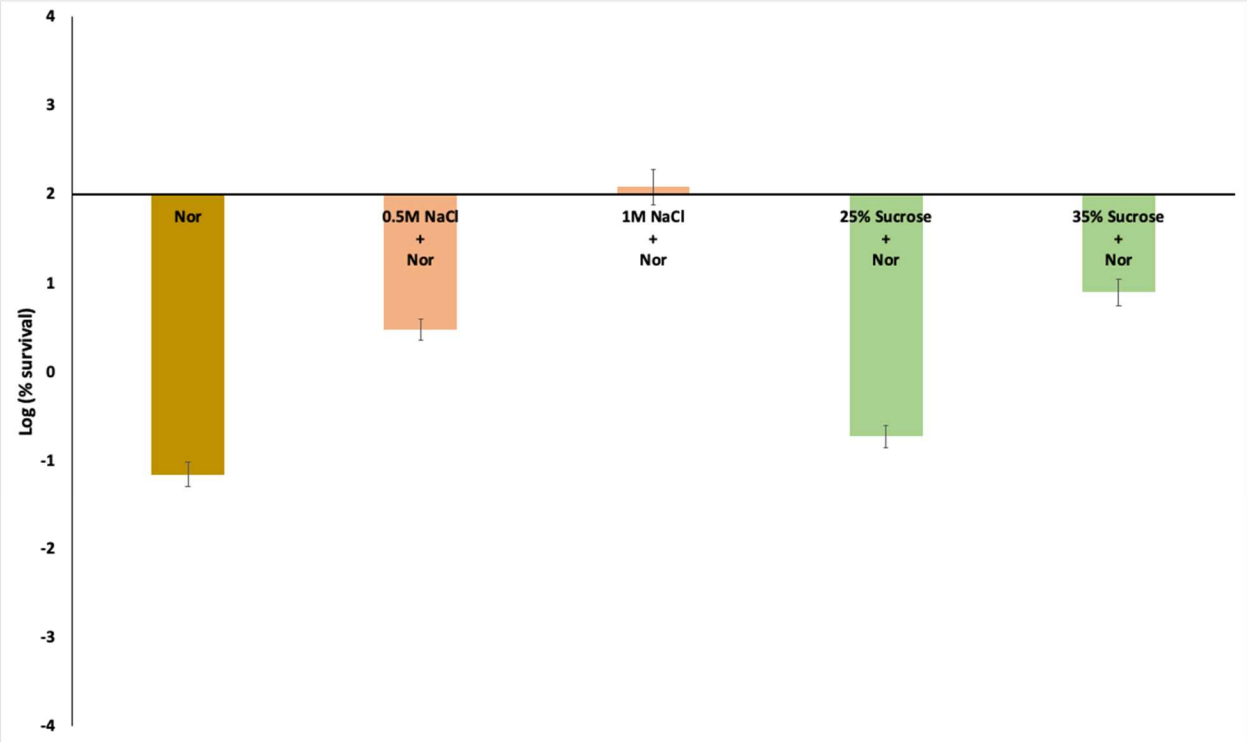

Figure 2.4 - Exposure to osmolytes increases *E. coli* survival to 1 µg/mL norfloxacin. The plot shows log percent survival of cells in Control (+ Nor), 0.5M & 1M NaCl (+ Nor), and 25% and 35% Sucrose (+ Nor). Control values for each condition are omitted as they are displayed in Fig 2.3. All log percent survival values are averages of viable CFUs after 4 h exposure with 1 µg/mL norfloxacin in 2 biological replicates and 2 technical replicates for each biological replicate in each condition. Error bars represent standard deviations.

2.4 Discussion

Studies demonstrating the cross-protective effects of osmotic stress are limited. The strongest phenotypic response has been demonstrated by MIC measurements, as cells exposed to NaCl experience up to a 4-fold increase in MIC across different classes of antibiotics [76]. Several studies have recently shown that tolerance phenotypes, on the other hand, exhibit orders

of magnitude enhancements in growth due to stress cross-protection [58,67]. Tolerance phenotypes have been shown to precede mutations that lead to genetic MIC-shifted resistance [56,58]. In an experimental model that attempts to explain tolerance, a high concentration of NaCl (0.4M) confers growth protection to bacteriostatic agents in an *E. coli* population by moderately sustaining the growth rate (from a ~60% drop to 35%) [35]. A limitation of this study is that it does not evaluate bactericidal antibiotics, which have greater clinical relevance as first-line therapy due to their efficacy against tolerant populations [36,77-80]. In addition, bacteriostatic antibiotics, similarly to osmolytes, disrupt metabolically active processes, thus providing little to no clinical efficacy on metabolically suppressed tolerant cell populations [54]. Bactericidal agents, however, increase metabolic demand and accelerate cellular respiration, responses which, when perturbed by osmolytes, provide valuable insight into the development of antibiotic tolerance [54].

Our results indicate that osmotic stress cross-protects *E. coli* K-12 substr. MG1655 against antibiotics. The osmolyte type (ionic vs. non-ionic) and antibiotic class influenced the magnitude of the induced tolerance phenotype. The osmolarity of the growth medium alone, however, did not explain the differences in the levels of cross-protection. For example, lower levels of osmotic stress, such as 0.25M NaCl (0.77 Osm/L) and 15% sucrose (0.71 Osm/L), had equivalent osmolarities but varying magnitudes of cross-protection in cells challenged by aminoglycosides. Higher levels of osmotic stress, however, such as 0.5M NaCl (1.27 Osm/L) and 35% sucrose (1.29 Osm/L), displayed similar degrees of cross-protection in cells challenged by β-lactam and fluoroquinolone antibiotics. These results suggest that the differences in the stress response systems of each osmolyte, along with the variations in response to the stress of different classes of antibiotics are useful indicators of cross-protection.

The higher levels of cross-protection of 0.25M NaCl with aminoglycosides indicate that cell responses which are sensitive to lower concentrations of salt stress may also be triggered under aminoglycoside stress. Additionally, around 40% of upregulated gene responses are not shared between NaCl and sucrose treatment, suggesting that genes upregulated in response to NaCl alone play a larger role in aminoglycoside cross-protection, whereas genes shared with sucrose or upregulated in sucrose alone do not cross-protect to the same degree [90]. Efforts to validate this theory utilizing RNA-Seq (Ranjbar, 2020, Chapter 5) revealed NaCl-aminoglycoside specific responses, which may explain the mechanisms behind stronger cross-protection, along with the activation of different, yet functionally related efflux pump systems derived from sucrose-aminoglycoside interactions. Among 300 genes which were significantly up- or down-regulated by osmotic stress, 43% of genes responded only to NaCl and 37% of genes were specific to sucrose [84]. Genes that we found were upregulated in response to both NaCl and aminoglycoside treatment included tolC, an outer membrane protein indicated in antibiotic efflux, and ompC and ompF, which are classified as outer membrane porin proteins that play a role in antibiotic uptake and are implicated in antibiotic tolerance and resistance. Efflux pump expression is higher in tolerant cells which leads to more effective pumping out of the drug [92]. Although we found these responses to be specific to aminoglycoside tolerance, these genes are also implicated in tolerance and resistance to β-lactam and fluoroquinolone antibiotics [33,91,92]. Responses to sucrose and aminoglycoside treatment, however, involved upregulation of the CusCFBA, AcrD, and AcrEF efflux pump systems [84]. While the role of these pumps in tolerance is not well understood, the interactions between these systems are shared with proteins that are implicated in tolerance, such as tolC. For example, the functional complexes of AcrAD-TolC and AcrEF-TolC play a role in multidrug efflux of aminoglycosides,

β-lactams, and fluoroquinolones [93]. The results of these experiments suggest that efflux activity may be a suitable mechanism of cross-protection The associations derived from genotypic sequencing, paired with phenotypic survival assays, show that enhanced efflux activity may be one of many mechanisms involved in cross-protection.

Antibiotic tolerance is generally associated with physiological dormancy, though recent efforts in understanding tolerance mechanisms demonstrate that tolerant cells undergo active protein and DNA synthesis [33]. In addition, our time-kill survival assays show that cross-protected cells undergo active DNA replication, albeit at a slower rate. This is likely due to the induced metabolic rate increase of bactericidal antibiotics, paired with the ability of cells to buffer against osmotic changes to continue growth [50,54]. Therefore, mechanisms that attempt to explain osmotic stress-induced cross-protection may need to account for the antibiotic entry and killing pathways and how these pathways may be perturbed under osmotic stress. Most conventional antibiotics kill by corrupting metabolism-dependent targets [94]. For example, aminoglycosides cause mistranslation, which produces toxic misfolded peptides that damage the membrane [95]. β-lactams kill cells for forcing peptidoglycan synthesis, and fluoroquinolones act by stabilizing gyrase-DNA intermediates which release lethal double-strand DNA breaks [94]. These mechanisms of killing occur after antibiotic entry, which is primarily influenced by membrane permeability and efflux activity. Hydrophobic antibiotics, such as aminoglycosides, enter the cell membrane by metabolic activity-dependent diffusion, while hydrophilic antibiotics, such as β-lactams and some fluoroquinolones, enter through porin channels such as OmpF and OmpC [92].

The mechanism of cellular entry with aminoglycosides is unclear, but the bactericidal effects are well studied and attributed to mistranslated proteins causing membrane pores that leak ions, which in effect forces cells to generate a voltage-dependent MP correlated with subsequent cell death [95]. While voltage is required for bactericidal activity, the lack of MP does not prevent aminoglycoside uptake, protein mistranslation, and membrane destabilization [95]. In line with this mechanism, NaCl treatment has been shown to dissipate MP through disruption of metabolism brought on by depolarization, which involves transporting Na^+ inside the cell through energetically unfavorable processes [96]. Thus, interchangeable energy-dependent processes between NaCl and aminoglycosides may confer cross-protection. These processes are intrinsically tied to metabolism, and disruption of metabolism interferes with MP which enables cells to become tolerant to antibiotics [95]. While cell responses to sucrose, β-lactams and fluoroquinolones are also tied to metabolism, the mechanisms behind which they influence metabolic activity and perturb MP needs further investigation [33,97].

CHAPTER 3 – INVESTIGATION INTO MECHANISMS OF CROSS-PROTECTION

3.1 Introduction

Antibiotic tolerance is distinguished by suppressed metabolism, whereas the efficacy of antibiotic treatment is strongly dependent on an active bacterial metabolic state [19,98,99]. The links between metabolic state and efficacy has been demonstrated for aminoglycoside, β-lactam, and fluoroquinolone antibiotics [54,98,100]. The strong metabolic dependency of these antibiotics limits their efficacy in chronic and recurrent infections, and as such there has been growing interest in developing techniques to probe cell metabolic state during antibiotic treatment [54,98,100]. However, efforts to mechanistically investigate metabolism have been limited to targeted measurements of metabolic states at single time points, disregarding the dynamic responses of cells that evolve interdependently [26,29,55,101].

The interdependence of cellular metabolic responses has resulted in various mechanisms explaining the onset of antibiotic tolerance. Many of these explanations point to the components of oxidative phosphorylation by decreases in its substrates, such as NADH, and products, such as ATP, as reliable determinants of a tolerant metabolic state [54,94,102]. Tolerance is also explained through downshifts in energy-generating intermediates in the TCA cycle [26,29,55]. More recent observations suggest that perturbations in PMF-dependent membrane energy states, which include the MP and proton gradient across the membrane, precede the onset of tolerance [34,103]. In fact, polypeptide and aminoglycoside killing depend on membrane activation by hyperpolarization, while membrane deactivation, or depolarization, is responsible for tolerance onset [95,104-107]. Thus, tolerant cells may accumulate antibiotics, as uptake is not dependent on PMF, and subsequently increase efflux while maintaining a low metabolic state. Efflux pumps span the membranes of both Gram-negative and Gram-positive species, and upregulation of efflux genes play an active role in conferring tolerance after antibiotic uptake [33,92]. In addition to efflux, tolerance involves influx of ions through the activity of the sodium/proton antiporters, which facilitate the movement of positively charged Na^+ ions into the negatively charged cell, further contributing to depolarization of the membrane [108]. In fact, cells challenged by NaCl, an ionic osmolyte, sustain membrane depolarization due to Na^+ influx and K^+ efflux, suggesting another possibility of a shared mechanism in the relationship between osmotic stress and antibiotic tolerance [90].

Metabolic assays generally provide readouts of specific components of metabolic activity as indicators of tolerance, such as ATP levels, NAD^+/NADH ratios, oxygen consumption rate, and MP. More recently, metabolic profiling and gene expression assays have been used to identify key metabolites and metabolic pathways involved in antibiotic tolerance [54]. These assays are sensitive and reliable determinants of bacterial metabolism, but due to the limitations of destructive sample preparation methods, multiple measurements and duplicative growth culture conditions are necessary in order to draw viable conclusions. Consequently, this introduces variables such as colony-to-colony variation and sampling errors, especially when testing across multiple culture conditions and timepoints. In addition, the per-sample cost of running these assays can be burdensome and require expensive equipment and facilities to store samples at varying temperatures. This may prove troublesome in a clinical setting, as physicians do not have a robust method for diagnosing tolerance and often have to outsource sample testing to 3rd party laboratories. Thus, there exists a need to develop assays which are low-cost to perform, do not require costly machinery and facilities, are non-destructive, and provide readouts

of dynamic metabolic changes in cell populations. As such, we propose utilization of the resazurin reduction assay, a fluorescent dye that is reduced intracellularly to fluorescent resorufin, to measure cell metabolism in evaluating antibiotic tolerance.

The resazurin reduction assay is commonly used as a tool in industrial dairy farming as an indicator of bacterial and yeast contamination in milk [109]. In recent years, the assay has been utilized for screening antimicrobial activity, cytotoxicity, and antibiotic resistance [110-113]. Notably, the assay is dependent on the ability of actively metabolizing bacteria to reduce the redox-sensitive dye, producing a change in color from blue to pink. Bacterial reduction of resazurin is dependent on diffusion into cells, where it is reduced by membrane-bound and cytosolic dehydrogenases, such as NADH-dependent oxidoreductase [114]. Once resazurin is reduced to the fluorescent product, it is then excreted into the medium where the fluorescence is measured by a spectrophotometer [114]. Thus, cellular processes involved in resazurin reduction require active metabolic processes, such as efflux and maintenance of MP. Additionally, resazurin reduction rate has been shown to be correlated with intracellular NADH levels, suggesting that the assay can be used to track cellular respiration [115]. Therefore, we propose that the resazurin reduction assay is a reliable technique to distinguish between metabolic states in cells that are: (1) susceptible to antibiotics, (2) osmotically stressed, (3) osmotically stressed and antibiotic tolerant, and (4) antibiotic tolerant without osmotic stress.

3.2 Materials and Methods

3.2.1 Resazurin Reduction Assay

The bacterial strains were cultivated according to the conditions in 2.2.1, but with a starting experimental cell density of 0.1 OD. Samples were loaded in triplicates into flat bottom 96-well plates (Caplugs Evergreen) with lids on to prevent evaporation. The outer wells of the plate were loaded with water in replace of sample to maintain sensitivity of the assay and reduce noise due to evaporation, otherwise known as the “edge effect”. Each sample well was filled with 5 uL of 1 mg/mL resazurin (Thermo Fisher) dissolved in PBS, bacterial culture, and/or antibiotics and osmolytes (2.2.1). Resazurin and resorufin spectral and fluorescence analysis conditions were adopted from our previous work [116]. In brief, 96-well plates were placed in a microplate reader (Thermo Fisher Scientific, Varioskan LUX Multimode Microplate Reader) and shaken at 300 rpm high force and 37˚C for several hours depending on the experiment setup. Readings were collected every 5 minutes at the predesignated settings: OD 680 nm; resazurin fluorescence with excitation bandwidth 615 nm, emission bandwidth 635 nm; resorufin fluorescence with excitation bandwidth 490 nm, emission bandwidth 585 nm.

3.2.2 Data Analysis

Raw experimental readings of samples in triplicates were averaged and rate of reduction was calculated by subtracting the latter averaged reading with the former, or:

$$ft= dydt = yt+5-y(t)5$$

where *y* is the measurement collected and *t* is the time from the start of measurements. To reduce noise due to equipment error, we calculated a 5-point running average of the rates, specifically the averages of the two data points before and after, inclusive of the time point. This is represented as:

Ft= t-10t+10ft5

where F(x) is the final output of the data.

Sample data was corrected for background noise by adjusting experimental sample wells against growth media and resazurin only wells. The correction was calculated using the formula:

Corrected t=R0-(Rot-Rt)

where Corrected(t) is the corrected value of the resazurin fluorescence; R(0) is fluorescence at t = 0; $R_0(t)$ is fluorescence of the background group (wells with only M9) at time t; and R(t) is the fluorescence at t. Only the corrected values of readings will be displayed in 3.3.

3.3 Results

To validate intracellular resazurin reduction as an indicator of metabolic state, our previous work demonstrated reduction rate of resazurin as a function of time [116]. We showed that resazurin reduction is sensitive to culture density (**Fig 3.1A, B)**, while resazurin reduction rate resolves fluctuations in reduction and normalizes to culture growth (**Fig. 3.1C**).

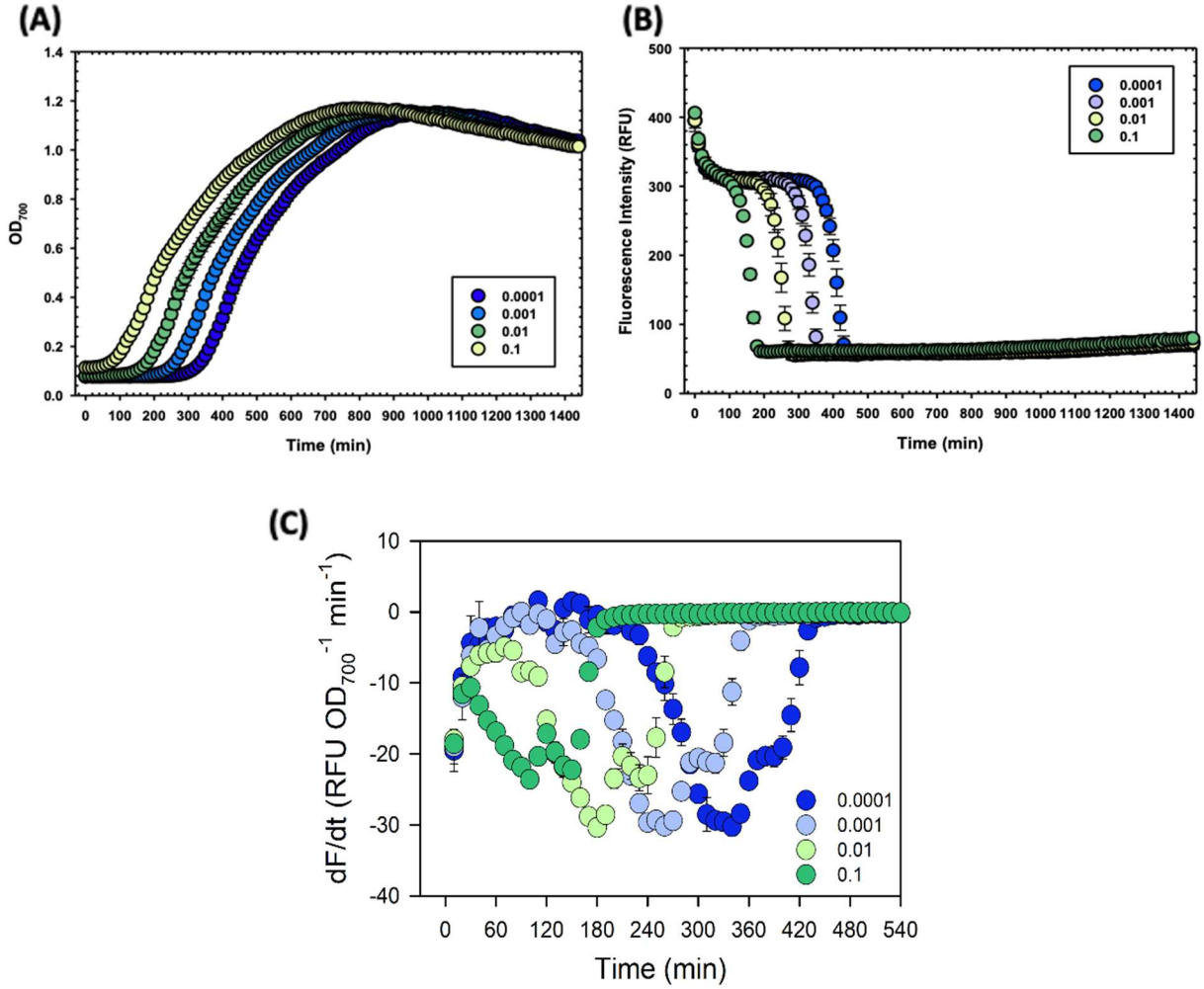

Figure 3.1 - Resazurin reduction displays metabolic activity in bacterial populations under different inoculum densities. Growth curve (A) and resazurin fluorescence (B) of *E. coli* MG1655 cultures growing in LB from varying starting inoculum densities (OD_{600}). Resazurin reduction rate (C) provides short timescale characterization of population level metabolic activity, displayed by derivative fluorescence plots. Values in the legend correspond to optical density at 700 nm of starting experimental cultures. Graphs are adopted from Rojas-Andrade & Hochbaum (2022) [116].

Thus, evaluating resazurin reduction rate over short timescales is highly informative and can be used as a tool to track metabolic responses of cell populations to osmotic stress.

3.3.1 Resazurin reduction rate of *E. coli* MG1655 challenged with bactericidal antibiotics

We first established the reduction rate of cells exposed to concentrations above and below the LCL of Kan, Tob, Amp, and Nor. To best capture the highest rate of metabolism over the duration of the assay, the starting density of bacterial cells used (after a 4 hr subculture) was 0.1 OD. Cell densities below 0.1 OD did not resolve distinguishing peaks in reduction rate between samples, and densities above 0.1 OD included a larger percentage of cells in the population that were mature and less active metabolically (data not shown). Cell populations exposed to the aminoglycoside Kan experienced accelerated metabolism at all concentrations,

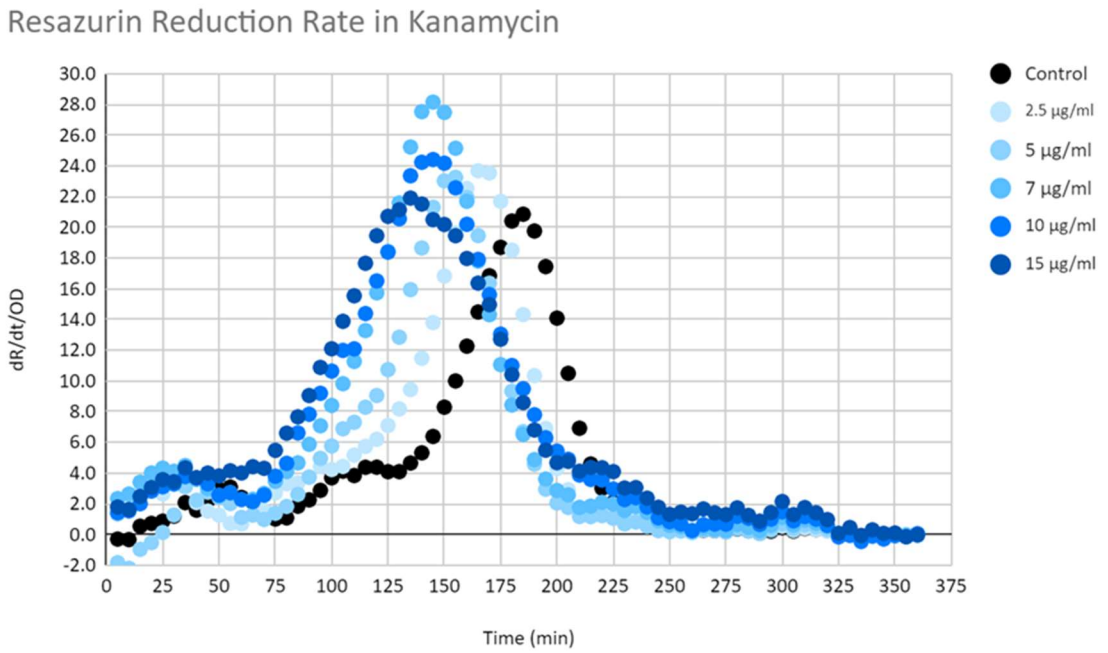

Figure 3.2 - Resazurin reduction rate in *E. coli* MG1655 exposed to kanamycin. Resazurin reduction rates of cell populations exposed to 2.5-15 µg/mL kanamycin, displayed by derivative fluorescence plotted on Y-axis, and time plotted on X-axis. Values and colors in the legend correspond to concentrations of antibiotic used. Reduction of control cells not exposed to kanamycin is visualized by the black dotted curve.

Indicated by an earlier reduction rate peak relative to control populations (**Fig. 3.2**). Similar to Kan, cells exposed to Tob experienced an earlier peak in reduction across all concentrations relative to control (**Fig. 3.3**).

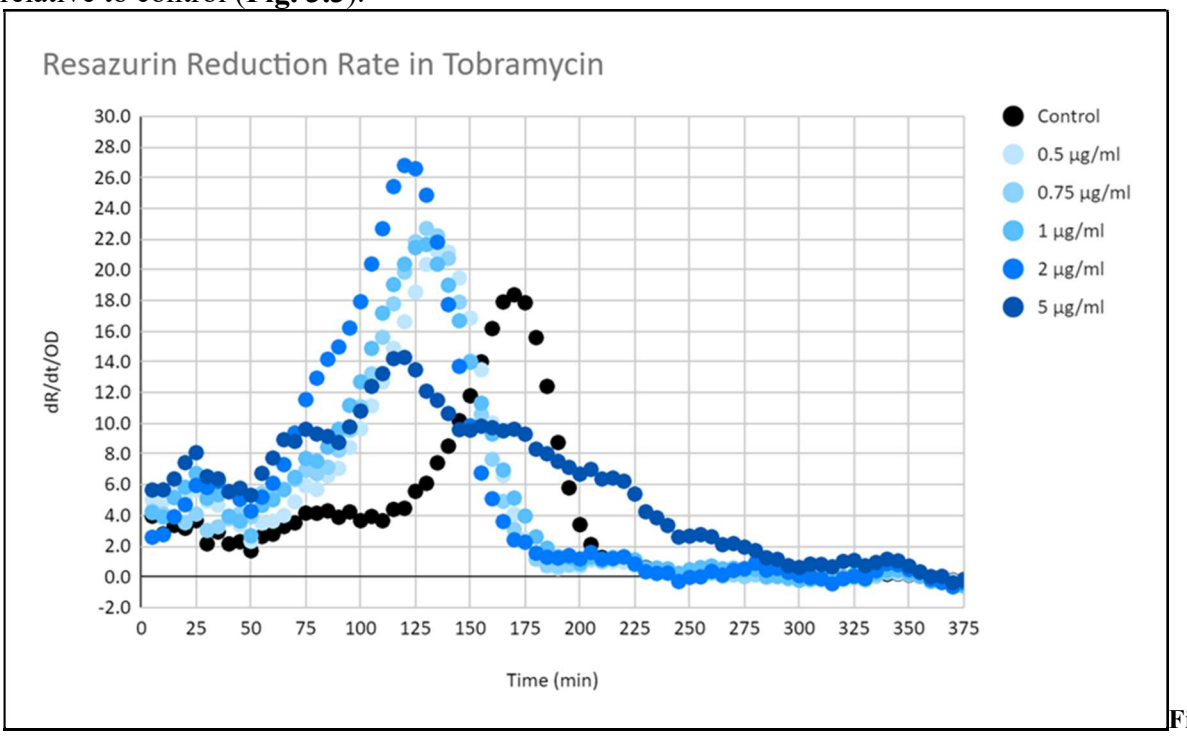

Figure 3.3 - Resazurin reduction rate in *E. coli* MG1655 exposed to tobramycin. Resazurin reduction rates of cell populations exposed to 0.5-5 µg/mL tobramycin, displayed by derivative fluorescence plotted on Y-axis, and time plotted on X-axis. Values and colors in the legend correspond to concentrations of antibiotic.

Next, we evaluated resazurin reduction rates of cells exposed to the β-lactam, Amp, and the fluoroquinolone, Nor, in concentrations below and above their respective LDLs. Cells challenged by Amp experienced similar levels of resazurin reduction at 5 and 10 µg/mL, respectively, when compared to control (**Fig. 3.4**). Exposure to 20 µg/mL Amp slightly slowed metabolism, indicated by a later reduction rate peak relative to control. At 40 µg/mL Amp, or the LDL, and above, there was no clear resazurin reduction peak, indicating low to no metabolic activity. However, at 40 µg/mL and above, there exists a slight upshift in reduction rate at 25-50 minutes which does not recover at later time points (**Fig. 3.4**). Cells challenged by Nor experienced a distinct acceleration in metabolism and increase in reduction rate at 2 µg/mL at 50 mins, whereas cells exposed to the lower concentrations of 1 µg/mL, the LDL, and 0.5 µg/mL have a slight acceleration in metabolism at 75-100 mins (**Fig. 3.5**). These results suggest that the resazurin reduction assay can distinguish between metabolic responses between the three classes of bactericidal antibiotics.

3.3.2 Resazurin reduction rate of *E. coli* MG1655 exposed to osmolytes

To determine the metabolic consequences of osmotic stress on cells using the resazurin

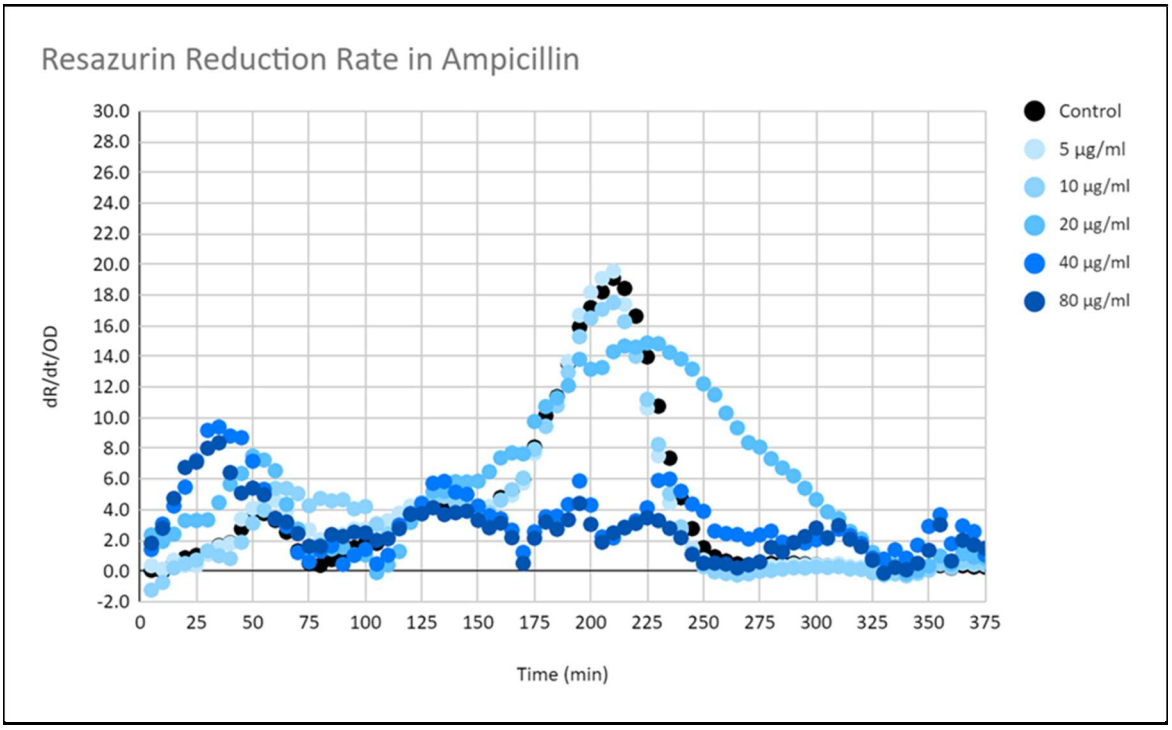

Figure 3.4 - Resazurin reduction rate in *E. coli* MG1655 exposed to ampicillin. Resazurin reduction rates of cell populations exposed to 5-80 µg/mL ampicillin, displayed by derivative fluorescence plotted on Y-axis, and time plotted on X-axis. Values and colors in the legend correspond to concentrations of antibiotic.

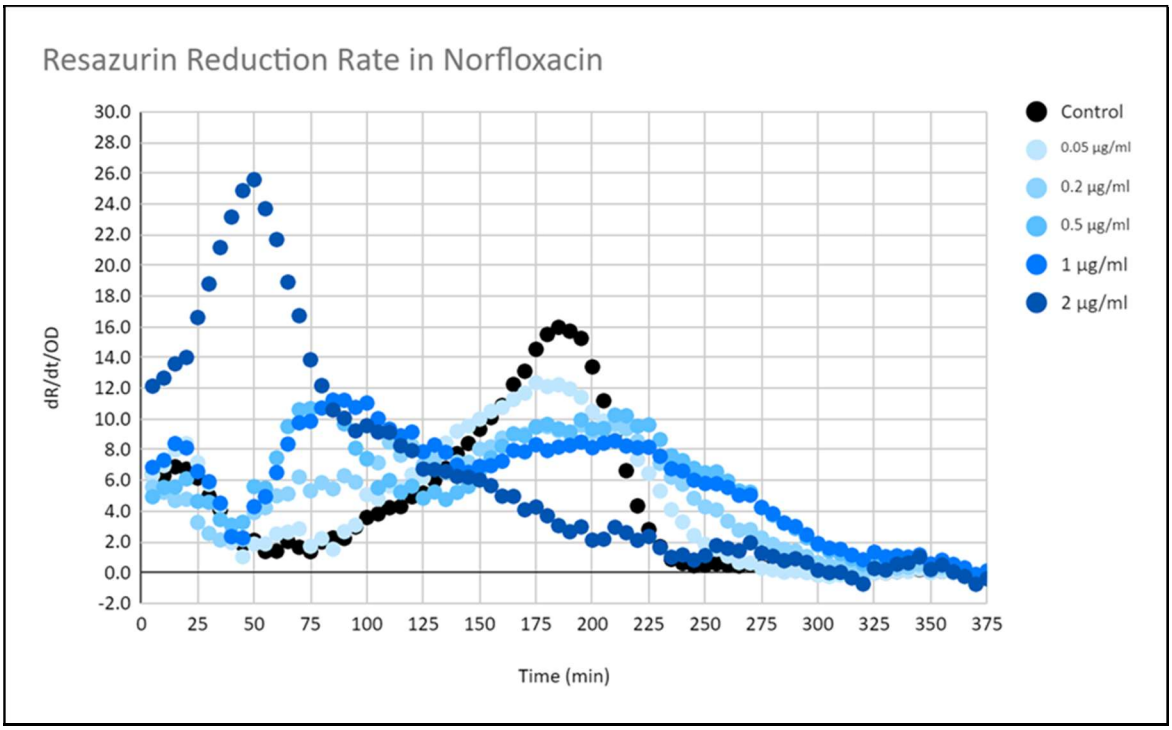

Figure 3.5 - Resazurin reduction rate in *E. coli* MG1655 exposed to norfloxacin. Resazurin reduction rates of cell populations exposed to 0.05-2 µg/mL norfloxacin, displayed by derivative fluorescence plotted on Y-axis, and time plotted on X-axis. Values in the legend correspond to concentrations of antibiotic.

reduction model, we exposed cells to a range of concentrations of NaCl and sucrose. Concentrations at and below 0.30M NaCl did not show any distinguishing features when compared to control, and concentrations above 0.50M NaCl displayed suppressed metabolism (data not shown). Therefore, we assessed the reduction rate in concentrations between 0.30M and 0.50M. At 0.35M and above, cell populations experienced delayed reduction rate peaks, indicating slowed metabolism (**Fig. 3.6**). The highest concentration of NaCl, 0.5M, showed the greatest delay in reduction rate peak when compared to control.

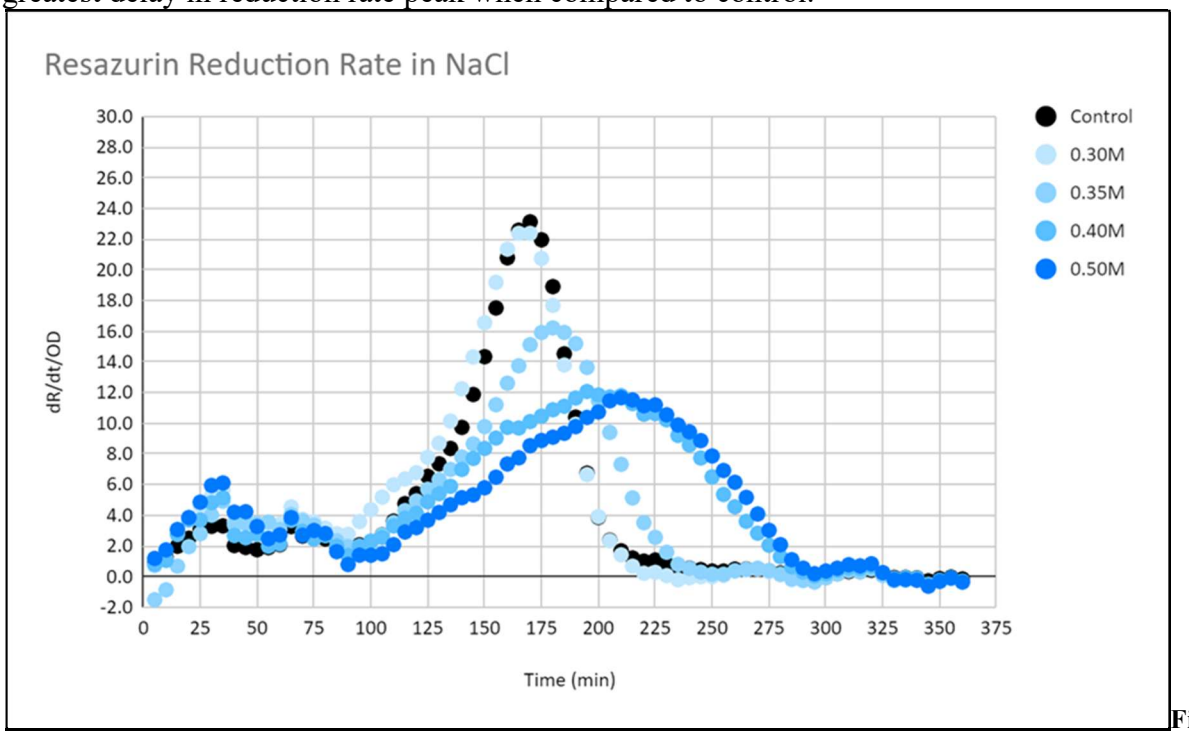

Figure 3.6 - Resazurin reduction rate in *E. coli* MG1655 exposed to NaCl. Resazurin reduction rates of cell populations exposed to 0.30-0.50M NaCl, displayed by derivative fluorescence plotted on Y-axis, and time plotted on X-axis. Values in the legend correspond to concentrations of osmolyte.

Populations exposed to sucrose were evaluated at concentrations above 15%, as concentrations below that had no effect on resazurin reduction rate (data not shown). Similarly to NaCl, the reduction rate in cells supplemented by 15-30% sucrose showed a delay in metabolism, accompanied by slowed metabolism (**Fig. 3.7**). Unlike NaCl treatment, however, reduction rates across all concentrations of sucrose were elevated, suggesting that mechanisms underlying the metabolic downshifts in resazurin reduction with NaCl and sucrose supplementation may be unique.

3.3.3 Resazurin reduction rate is correlated to antibiotic tolerance in cells co-exposed to antibiotics and osmolytes.

To determine whether antibiotic and osmolyte co-exposure shows a tolerant metabolic

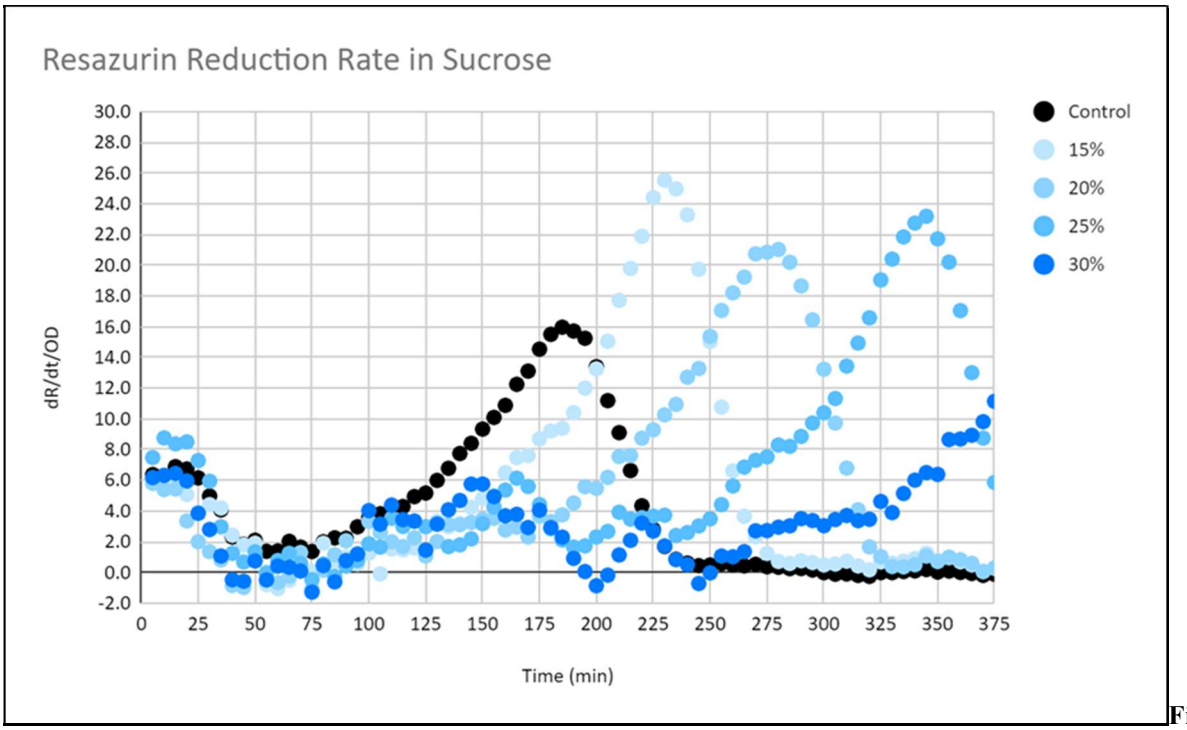

Figure 3.7 - Resazurin reduction rate in *E. coli* MG1655 exposed to sucrose. Resazurin reduction rates of cell populations exposed to 15-30% sucrose, displayed by derivative fluorescence plotted on Y-axis, and time plotted on X-axis. Values in the legend correspond to concentrations of osmolyte.

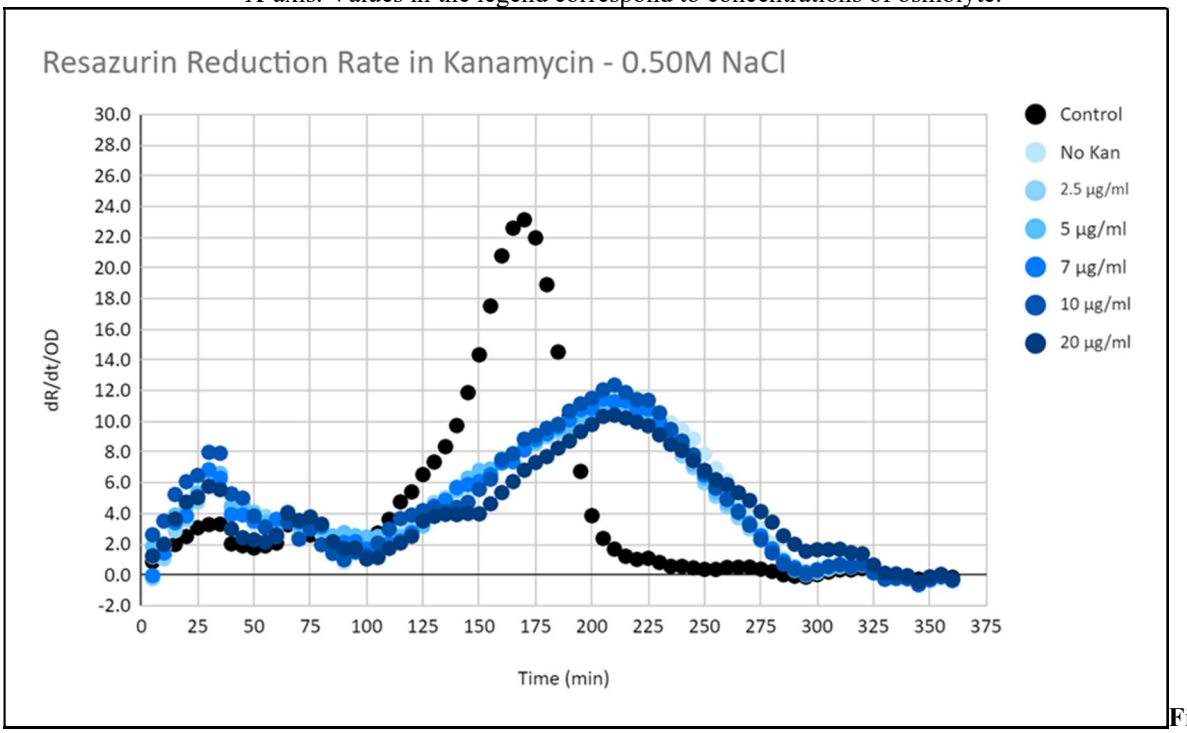

Figure 3.8 - Resazurin reduction rate in *E. coli* MG1655 exposed to NaCl and kanamycin. Resazurin reduction rates of cell populations exposed to 0.5M NaCl and 2.5-20 µg/mL kanamycin, displayed by derivative fluorescence plotted on Y-axis, and time plotted on X-axis. Values in the legend correspond to concentrations of antibiotic.

phenotype, we challenged cells to a single concentration of osmolyte against a range of antibiotic concentrations. We referenced the results of the survival assay discussed in 2.3 to determine the concentrations of osmolytes that would have the greatest survival effect on cells. Cells co-exposed to the aminoglycosides Kan and Tob (data for Tob not shown), along with 0.5M NaCl experienced a shift in resazurin reduction that overlapped to reduction in cells treated to NaCl alone (**Fig. 3.8**). The metabolism accelerating effect in cells during antibiotic-only treatment was not sustained during the co-exposure assay, indicating that NaCl has a greater influence on resazurin reduction. This trend in reduction was observed across all concentrations of antibiotic against NaCl. In cells co-exposed to Kan and Tob, along with 20% sucrose, resazurin reduction followed the same trend as NaCl as cell reduction was influenced more by sucrose relative to antibiotic (**Fig. 3.9**). However, unlike what was observed in Fig 3.8, cells co-exposed to sucrose and higher concentrations of antibiotic (10 and 20 µg/mL Kan) experienced suppressed metabolism with no clear peak in reduction rate. As this trend was not observed with reduction in 20% sucrose alone, this indicates a synergistic effect on reduction that is not observed with NaCl.

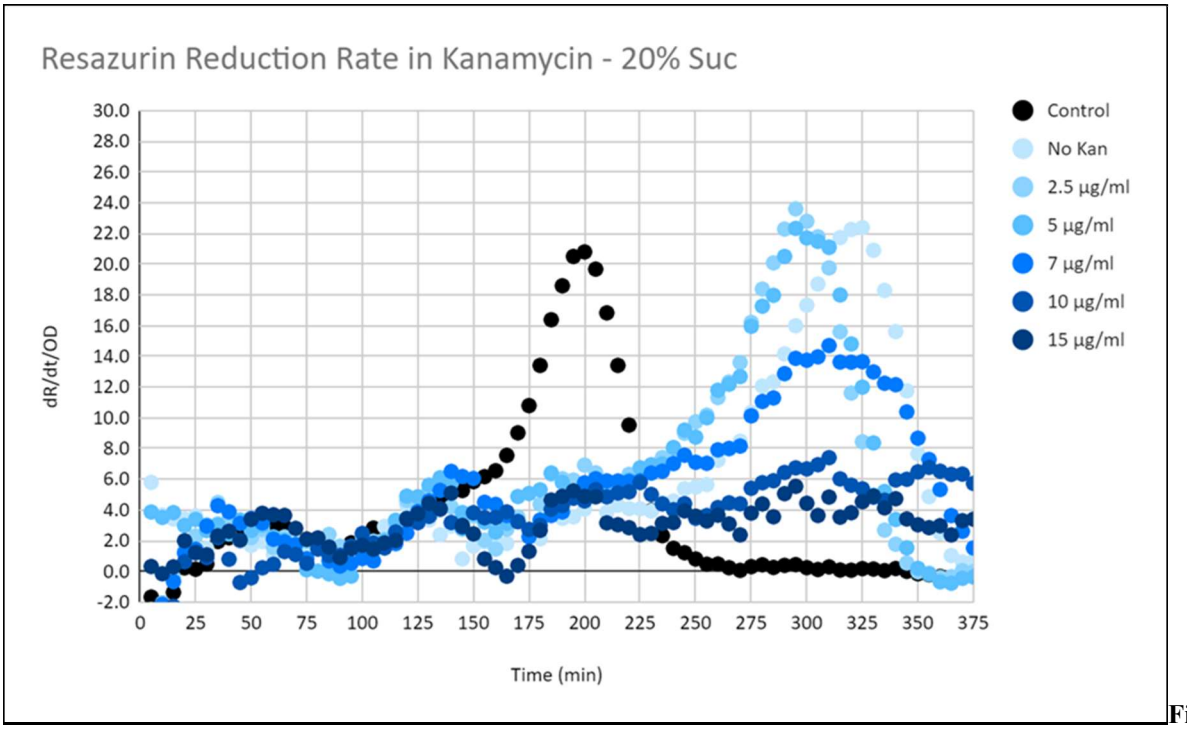

Figure 3.9 - Resazurin reduction rate in *E. coli* MG1655 exposed to sucrose and kanamycin. Resazurin reduction rates of cell populations exposed to 20% sucrose and 2.5-20 µg/mL kanamycin, displayed by derivative fluorescence plotted on Y-axis, and time plotted on X-axis. Values in the legend correspond to concentrations of antibiotic.

Cell populations co-exposed to Amp and 0.5M NaCl followed the same resazurin reduction trends as the aminoglycosides across all concentrations of Amp (**Fig. 3.10**). When

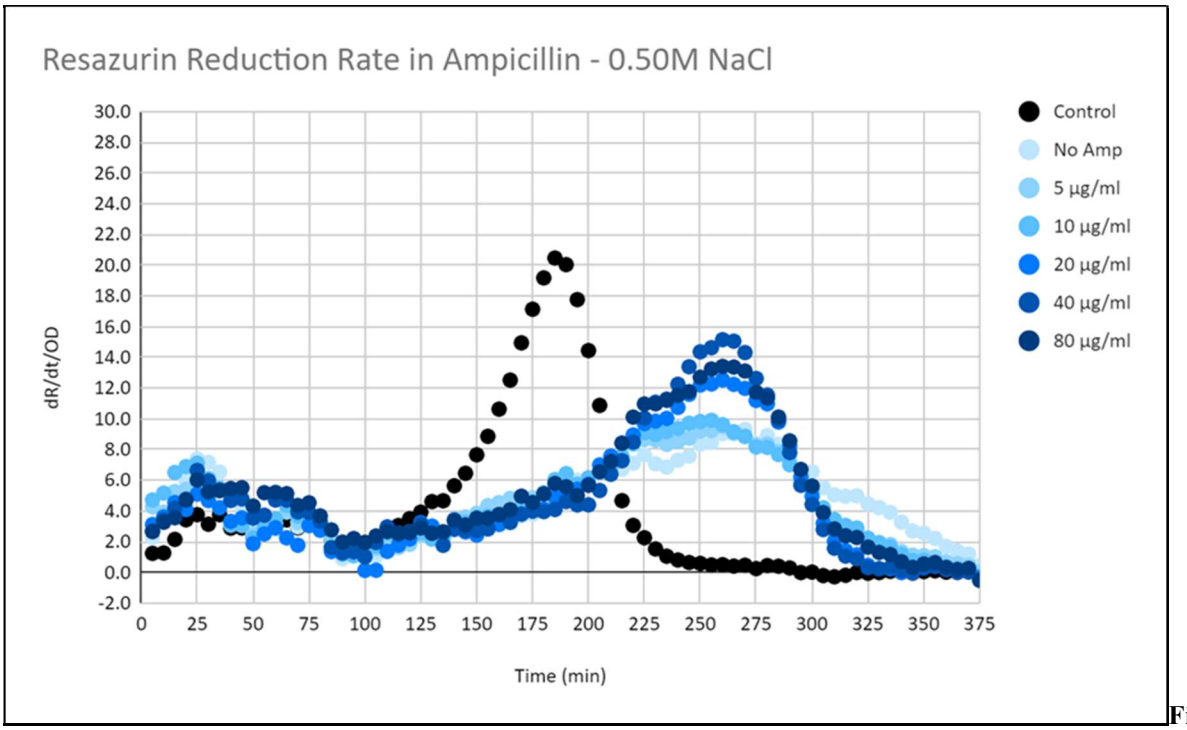

Figure 3.10 - Resazurin reduction rate in *E. coli* MG1655 exposed to NaCl and ampicillin. Resazurin reduction rates of cell populations exposed to 0.5M NaCl and 5-80 µg/mL ampicillin, displayed by derivative fluorescence plotted on Y-axis, and time plotted on X-axis. Values in the legend correspond to concentrations of antibiotic.

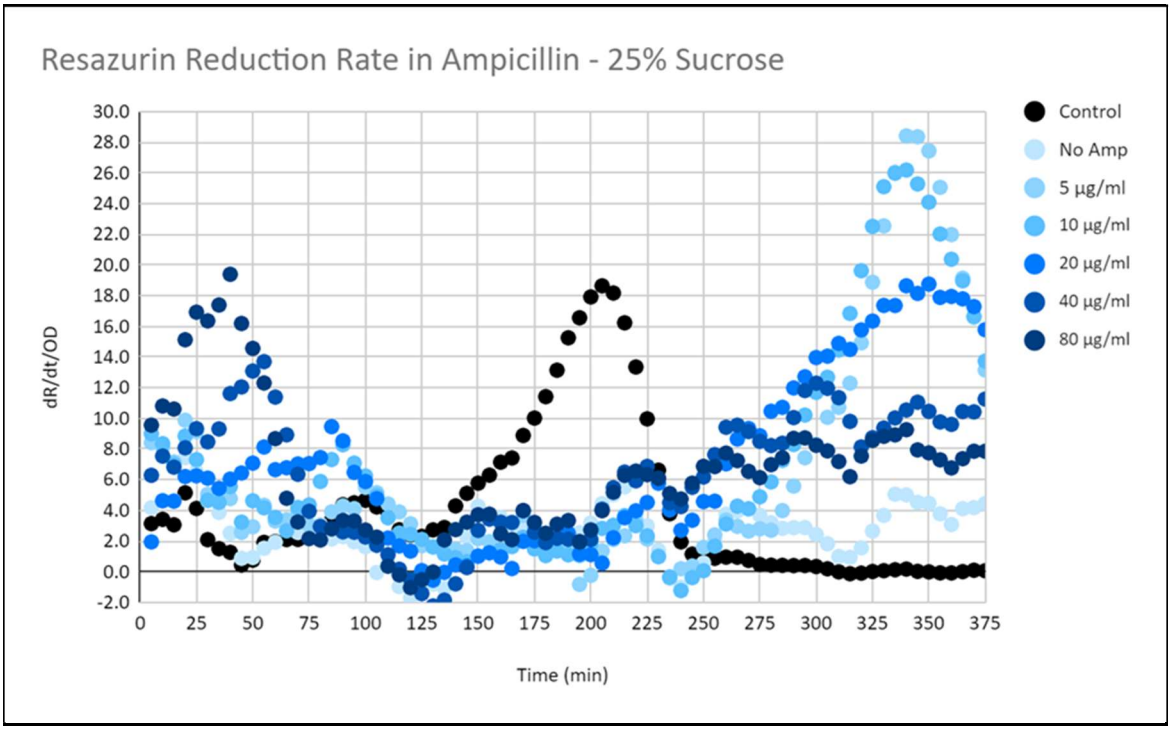

Figure 3.11 - Resazurin reduction rate in *E. coli* MG1655 exposed to sucrose and ampicillin. Resazurin reduction rates of cell populations exposed to 25% sucrose and 5-80 µg/mL ampicillin, displayed by derivative fluorescence plotted on Y-axis, and time plotted on X-axis. Values in the legend correspond to concentrations of antibiotic.

co-exposed to 25% sucrose and Amp, concentrations up to 20 µg/mL Amp had resazurin reduction peaks that occurred at similar time points (~340 mins) (**Fig. 3.11**). However, cells exposed to 40 and 80 µg/mL Amp and sucrose did not show comparable peaks in reduction rate at the same time point. Instead, a greater peak was observed with both of these concentrations at ~50 minutes relative to Amp treatment alone, indicating accelerated earlier metabolic activity that does not sustain at later time points (**Fig. 3.11**). Interestingly, NaCl addition did not display a strong influence on reduction rate when cells were co-exposed to Nor (**Fig. 3.12**). At concentrations of 0.2 µg/mL Nor and above, co-exposure with NaCl was not observed to influence the reduction rate. Reduction rate correlated with NaCl-only exposed cells when co-exposed with the lowest concentration of Nor, 0.05 µg/mL, suggesting that cell mechanisms of reducing resazurin are unique under Nor treatment and exhibit little to no overlap with NaCl mechanisms. This trend is also observed when cells are challenged by Nor and 25% sucrose, as only the lowest concentration of Nor, 0.05 µg/mL, and sucrose co-exposure results in reduction that is similar to sucrose reduction alone (**Fig. 3.13**). Furthermore, 2 µg/mL Nor and sucrose exposed cells maintain accelerated metabolism as observed through an earlier reduction rate, a trend which is also seen with NaCl and Nor. Thus, the mechanisms of resazurin reduction under both osmolytes are unique when compared to Nor reduction in cells.

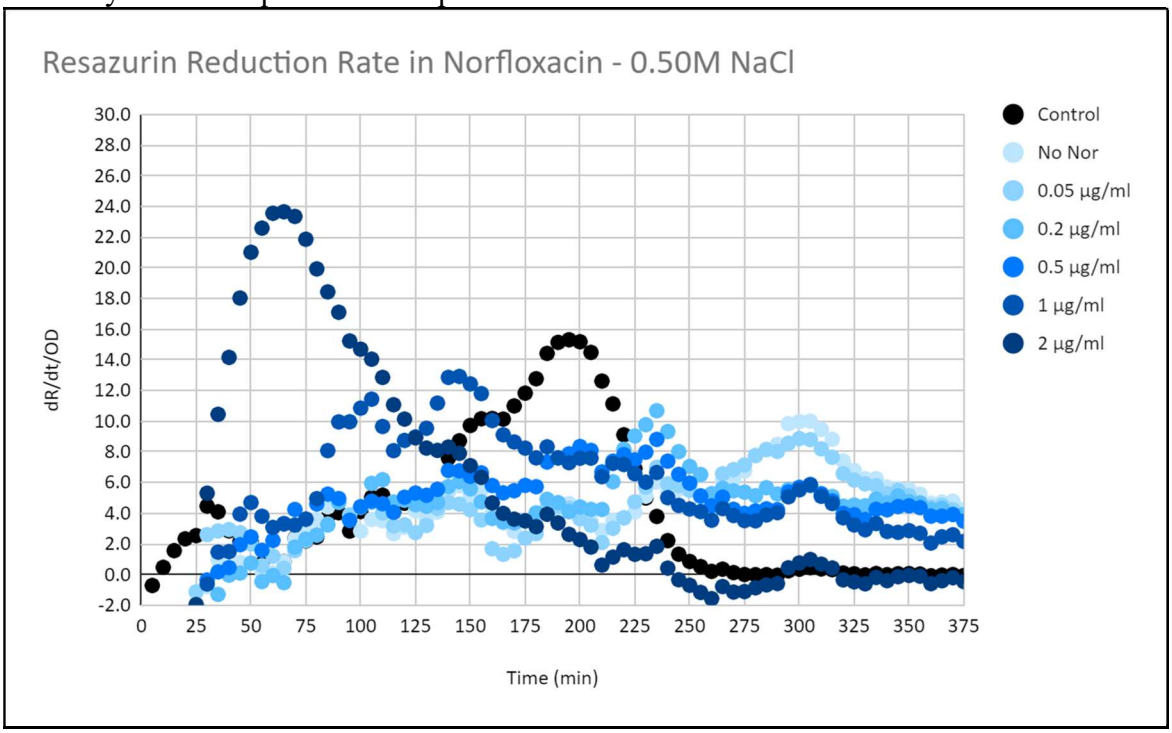

Figure 3.12 - Resazurin reduction rate in *E. coli* MG1655 exposed to NaCl and norfloxacin. Resazurin reduction rates of cell populations exposed to 0.5M NaCl and 0.05-2 µg/mL norfloxacin, displayed by derivative fluorescence plotted on Y-axis, and time plotted on X-axis. Values in the legend correspond to concentrations of antibiotic.

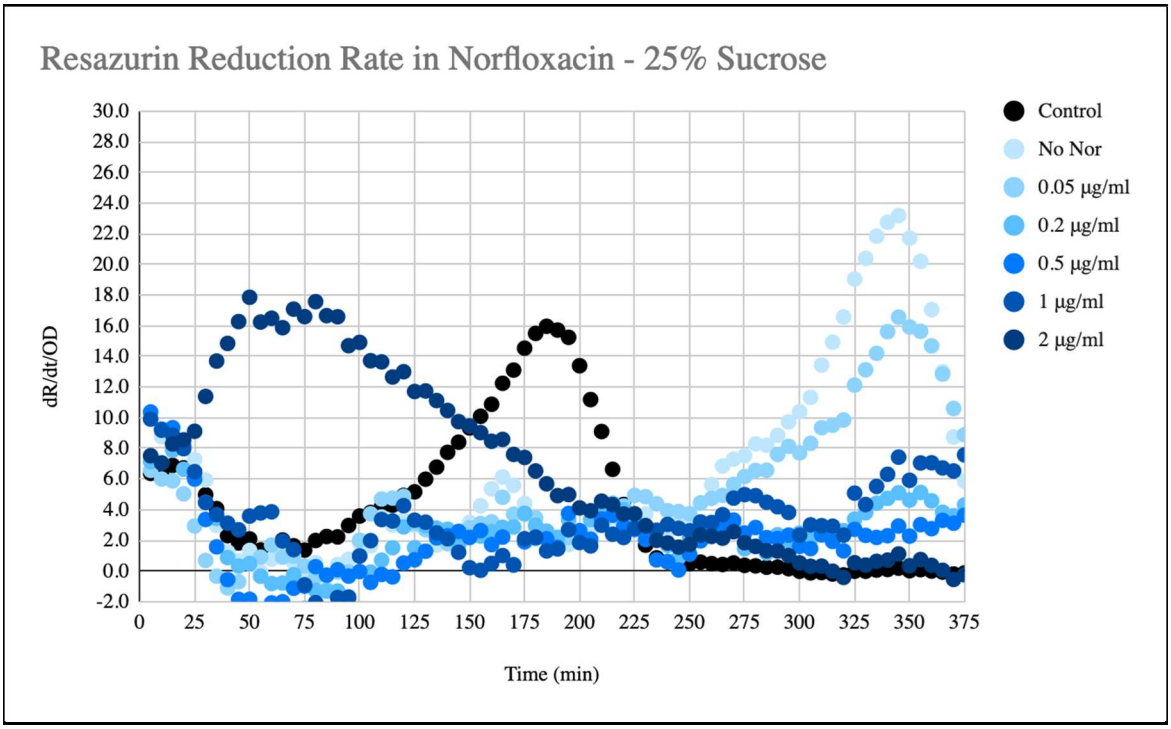

Figure 3.13 - Resazurin reduction rate in *E. coli* MG1655 exposed to sucrose and norfloxacin. Resazurin reduction rates of cell populations exposed to 25% sucrose and 0.05-2 µg/mL norfloxacin, displayed by derivative fluorescence plotted on Y-axis, and time plotted on X-axis. Values in the legend correspond to concentrations of antibiotic.

3.3.4 Dissipation of proton motive force shows similar resazurin reduction response when compared to NaCl

The proton ionophore cyanide m-chlorophenyl hydrazine (CCCP) depolarizes the cell membrane by dissipating voltage gradients. Depolarization, or deactivation, of the membrane is a factor responsible for antibiotic resistance and tolerance onset [95,104-107,117]. We challenged cells to CCCP, Kan, and CCCP + Kan to determine if CCCP slows metabolic acceleration by Kan as observed through a delayed resazurin reduction rate. Cells exposed to CCCP alone show a moderate delay in reduction as compared to control (**Fig. 3.14**). Cells that are simultaneously challenged with Kan and CCCP experience a delay in reduction relative to Kan-only exposed cells, suggesting that metabolism acceleration by Kan is blunted by CCCP addition. When cells are treated to both Kan and CCCP over a 4 hour period, survival is increased relative to Kan treatment alone (**Fig. 3.15**). Interestingly, although CCCP inactivates the cell membrane, it is not detrimental to cell growth, as cells experience a 1800% increase in growth over a 4 hr period. In fact, cell growth is maintained even during CCCP and Kan co-exposure with a 870% increase in growth over 4 hrs and a 1,800x factor increase in *E. coli* tolerance.

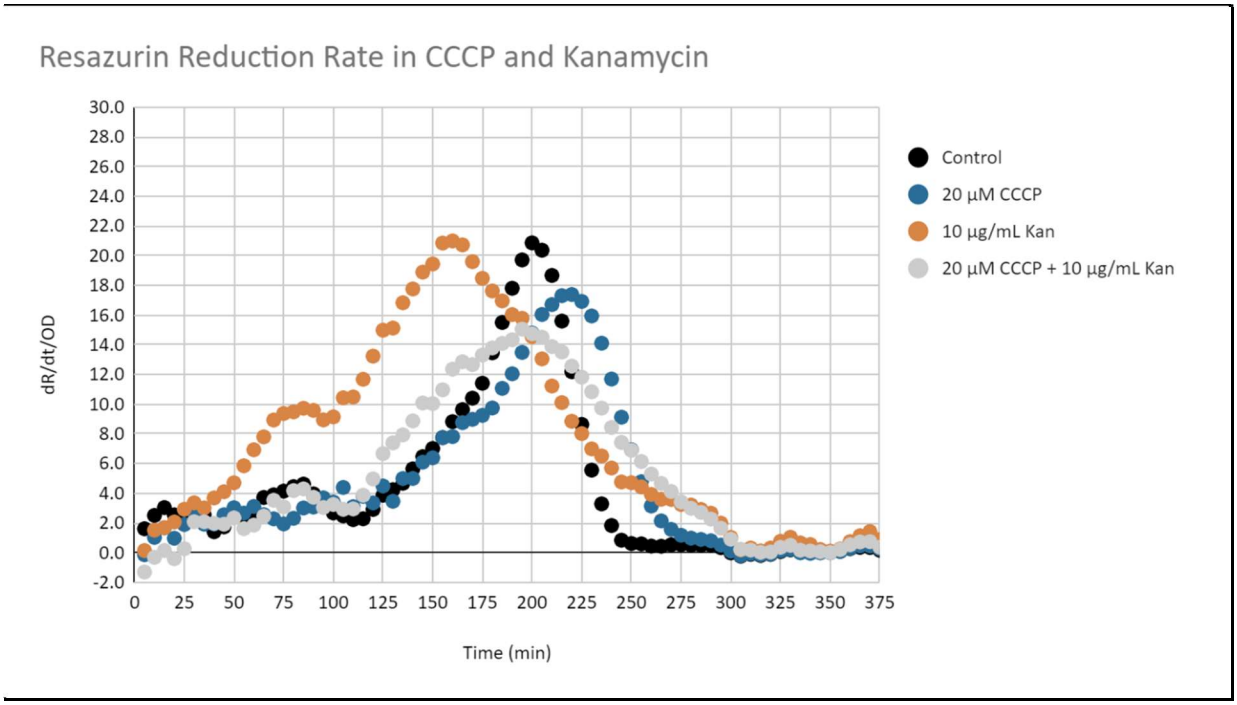

Figure 3.14 - Resazurin reduction rate in *E. coli* MG1655 exposed to CCCP and kanamycin. Resazurin reduction rates of cell populations exposed to 20 µM CCCP and 10 µg/mL kanamycin, displayed by derivative fluorescence plotted on Y-axis, and time plotted on X-axis. Values in the legend correspond to CCCP and kanamycin concentrations used.

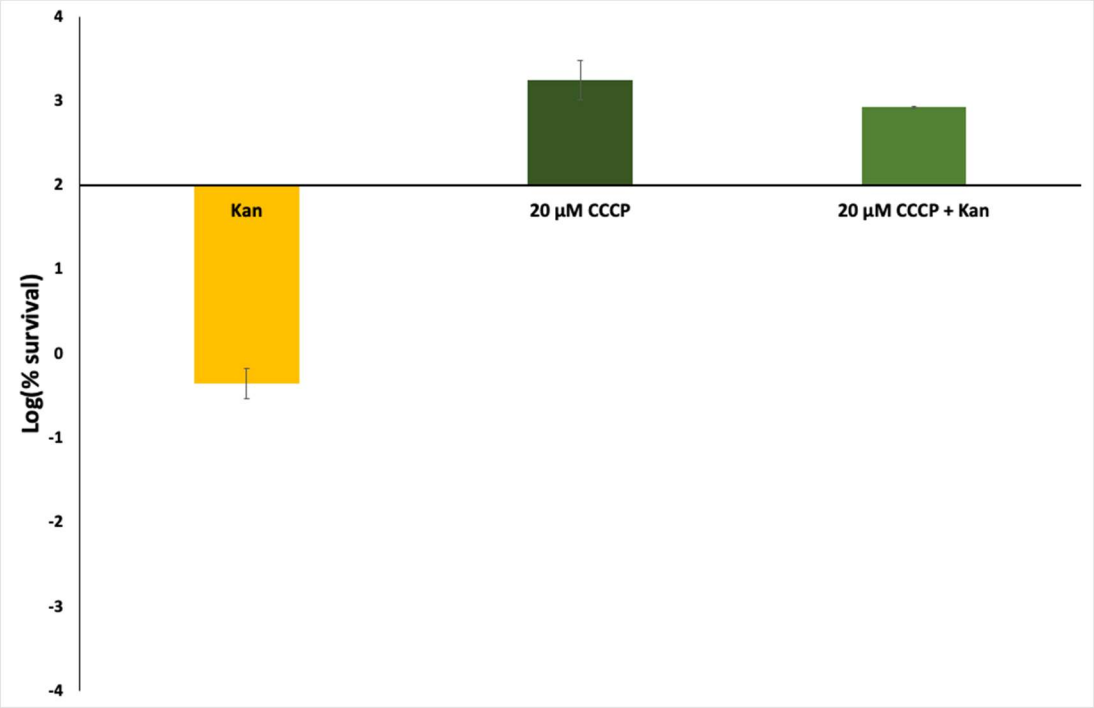

Figure 3.15 - Exposure to CCCP increases *E. coli* survival to 10 µg/mL kanamycin. The plot shows log percent survival of cells in Kan, and 20 µM CCCP (± Kan). All log percent survival values are averages of viable CFUs after 4 h exposure in 2 biological replicates and 2 technical replicates for each biological replicate in each condition. Error bars represent standard deviations.

3.4 Discussion

Antibiotic tolerance formation has been characterized by low ATP and NADH levels, decreased TCA cycle enzyme expression, reduced MP, and suppressed oxygen consumption rate [26,29,34,54,55,94,102,103]. These bioenergetic parameters can provide accurate quantification of metabolic activity, but techniques to measure them are destructive and require specialized equipment. Resazurin is an optically active dye that can undergo a two-electron reduction to resorufin, which causes a blue-shift of extinction spectra maximum and a decrease in resazurin fluorescence intensity. Resazurin is advantageous due to its low cost and practicality in utilizing the dye's reductive ability in tracking metabolism and antibiotic uptake through the various stages of cell growth [115,122]. Resazurin is found to be reduced by cytosolic and membrane-bound dehydrogenases and reductases, also referred to as diaphorases [114]. Diaphorases are widely distributed and found in many species from bacteria to mammals. In contrast to MTT, a colorimetric assay used to track metabolic activity, with a standard redox potential (E^{o}) of -110 mV, the standard redox potential of resazurin of +380 mV indicates that resazurin may also be reduced by cytochromes (E^{o} from +80 to +290 mV) [118]. Additionally, when tracking NADH content in response to antibiotic exposure, our lab has shown that resazurin reduction rate is correlated with intracellular NADH levels [115]. Thus, the resazurin reduction assay provides utility as a predictive marker for antibiotic tolerance. In this work, we show that resazurin reduction rate can be utilized as a metric for metabolic activity, and in turn be used to track antibiotic tolerance.

Impedance spectroscopy has recently been utilized to resolve MP fluctuations and is a robust technique for distinguishing between different life stages of bacteria. For example, *E. coli* membranes have been shown to experience a hyperpolarized MP of -220 mV in early exponential phase to a depolarized -140 mV in late exponential phase [120]. In NaCl exposure, positively charged Na^{+} ions utilize the electrochemical gradient favoring their movement into the negatively charged cell, resulting in depolarization of MP [90]. Under hyperosmotic stress, a switch from net K^{+} uptake to efflux becomes increasingly favorable, rendering the cell unable to compensate as Na^{+} ions outcompete K^{+} for binding sites in key cytosolic metabolic processes, causing a severe disruption to cell metabolism. Additionally, assays utilizing fluorescent dyes show that maximum depolarization of around -120 mV is reached, from -150 mV in mid-exponential phase, in cells treated to increasing concentrations of NaCl [90]. Thus, MP during NaCl supplementation resembles a less metabolically active state. In contrast, sucrose treatment leads to modest increases in net K^{+} uptake and hyperpolarization of MP [90,121].

The resazurin reduction of cells exposed to NaCl showed a trend indicative of suppressed metabolism, as reduction was delayed relative to control (**Fig. 3.6**). Comparatively, resazurin reduction in cells exposed to sucrose also displayed a trend of slowed metabolism, however, the magnitude of reduction rate was greatly heightened in these cell populations (**Fig. 3.7**). While the exact reason for a heightened or lowered reduction rate is not known, the metabolic consequences of osmolyte treatment are better understood and provide insight on cell response to osmotic stress. For example, similar to NaCl, depolarization is also experienced in cells challenged with CCCP, and resazurin reduction in cells subjected to individual exposure to both results in delayed reduction and lowered reduction rate (**Figs. 3.6 and 3.14**). On the other hand, metabolic consequences of cells in response to sucrose and aminoglycoside antibiotics may be shared to some extent, as the heightened reduction rate of cells challenged by sucrose correlates to the heightened rate in response to Kan and Tob (**Figs. 3.2, 3.3, and 3.7**). Cell responses to both of these types of stresses result in hyperpolarization of the membrane, perturbing metabolic

state [90,119,121]. Although the hyperpolarization effect may be shared, cell populations differ in their respective metabolic responses as they experience accelerated metabolism caused by Kan and Tob and slowed metabolism caused by sucrose, indicated by time of peak resazurin reduction rate (**Figs. 3.2, 3.3, and 3.7**) . Thus, we propose that resazurin reduction rate is a useful indicator of MP during periods of metabolic perturbation.

At a lower relative concentration of 0.5M NaCl, gene expression for efflux and porin protein coding genes are upregulated when co-exposed to gentamicin (see 2.4) [84]. However, depolarization of MP is observed at concentrations of NaCl as low as 0.1M [96]. Thus, cell exposure to both low and hyperosmotic concentrations of NaCl lead to depolarization of MP, but only hyperosmotic NaCl exposure leads to inactivation of efflux pumps. This may explain why the strong protection of NaCl, even at 0.25M, is observed with aminoglycoside survival, as the voltage-dependent processes required for aminoglycoside uptake and killing are perturbed (**Fig. 2.1**) [95]. While the literature behind the tolerance-inducing role of sucrose is unclear, it has been shown that frequent periods of hyperpolarization during growth increases efflux and promotes tolerance [121]. We predict that antibiotic efflux under sucrose exposure may include pathways that overlap with NaCl, but also include pathways that are unique, as roughly 40% of upregulated genes in *E. coli* share no similarity in their responses to NaCl and sucrose treatment [90]. One example demonstrating a contrasting response is seen when cells do not activate antiporters to extrude Na^+ from the cytosol during sucrose stress, whereas cells exposed to high concentrations of NaCl experience differential expression of genes that encode for antiporters NhaA, NhaB, and ChaA [90]. Interestingly, NhaA and ChaA are downregulated in NaCl exposed cells at a hyperosmotic concentration of 8% (~1.4M), but are indicated in tolerance to aminoglycosides, β-lactams, and fluoroquinolones as efflux pumps [33,90].

β-lactams and fluoroquinolones require active respiration for killing and enter through non-specific OmpF and OmpC porins, which are inactivated at voltages above their threshold potential [92, 123]. The minimum MP at which porins start to close are ~150 mV and ~200 mV for OmpF and OmpC, respectively, which exceed those that cells experience during NaCl depolarization and sucrose hyperpolarization [90,96,121,123]. Thus, there is no evidence that osmolytes are responsible for MP perturbations leading to decreased antibiotic uptake. Antibiotic efflux under Amp exposure is likely to occur, however, as cells exposed to a high concentration of Amp (50 μg/mL) experience hyperpolarized membrane voltages [121]. This may be attributed to the modest rise of reduction rate in 40 and 80 μg/mL Amp treated cells observed at 25-50 mins, and why a more pronounced rise in reduction rate is observed with sucrose but not NaCl addition (**Figs. 3.4, 3.10, and 3.11**). NaCl co-exposure with Amp, however, shows that cells experience depolarization and follow the reduction trend of NaCl-only cells (**Fig. 3.10**). Thus, tolerance to Amp is likely to be influenced by MP. The pronounced rise of reduction rate at 50 mins of cells exposed to 2 μg/mL Nor, 2 μg/mL Nor and NaCl, and 2 μg/mL Nor and sucrose suggest that cells exposed to Nor at high concentrations may experience hyperpolarization, yet co-exposure with osmolytes is not sufficient to impact MP (**Figs. 3.5, 3.12, and 3.13**). However, hyperpolarization of cells challenged by Nor has not been documented in literature and requires further investigation. Additionally, the dependency on metabolism for killing is slightly greater in Amp compared to Nor, as evidenced by the higher oxygen consumption rate and stronger ATP dependency requirements of Amp [54]. This may explain the greater cross-protection (**Figs. 2.3 and 2.4**) and metabolic influence of osmolytes in Amp exposed cells relative to Nor (**Figs. 3.10-3.13**).

The protective effects of NaCl during co-exposure is evidenced by repressed metabolic activity and increased efflux [47-49,84], while the protective effects of sucrose is evidenced only by increased efflux [121]. In addition, all of the antibiotics we tested require active respiration for killing, and while NaCl has been observed to disrupt cell metabolism independent of MP, it remains unclear if sucrose does the same [54,98]. Our results suggest that resazurin reduction is a sufficient indicator for antibiotic tolerance as indicated by metabolic perturbations in MP. We found that membrane depolarization by NaCl and hyperpolarization by sucrose are additional factors responsible for cross-protection, demonstrated by their greater impact on reduction relative to reduction under antibiotic exposure alone.

CHAPTER 4 – REPOTENTIATING TOLERANT CELLS TO ANTIBIOTICS AND FUTURE DIRECTIONS

Modulating metabolic activity through repotentiation to antibiotics is a viable strategy to enhance bactericidal drug-dependent killing. Resensitization to antibiotics was first implemented in antibiotic-tolerant *E. coli* and *S. aureus* populations, where gentamicin, an aminoglycoside, in combination with a variety of upper glycolysis metabolites (glucose, mannitol, and fructose) was shown to kill tolerant cells [77,127]. These metabolites increased PMF activity by activating the electron transport chain, thereby enhancing gentamicin uptake and killing. Additional studies sought to demonstrate repotentiation by combining various carbon sources, such as amino acids (e.g. alanine) and TCA cycle metabolites (e.g. pyruvate, citrate), with aminoglycoside antibiotics [124-126].

To determine if cells exposed to osmolytes can be repotentiated to antibiotics, we used a series of metabolites for co-exposure: fumarate, succinate, alanine, pyruvate, citrate, and acetate. All metabolites were purchased from Sigma-Aldrich. Resazurin reduction assays were utilized to track metabolic changes, such as MP perturbation, in cell populations. Conditions were then validated against survival assays to determine if resensitization to antibiotics occured. The only metabolites that resulted in a reduction shift were alanine and acetate (data not shown), marked by delayed reduction rates, and citrate, indicated by an earlier reduction rate peak (**Fig. 4.1**). Citrate was selected for its greater likelihood of inducing repotentiation. All citrate concentrations tested resulted in earlier reduction rate peaks, but 50 and 100 mM citrate displayed the greatest shift relative to control (**Fig. 4.1**). As discussed in sections 3.3 and 3.4, an earlier reduction rate peak is likely to correlate with accelerated metabolism, thus increasing the likelihood of repotentiation.

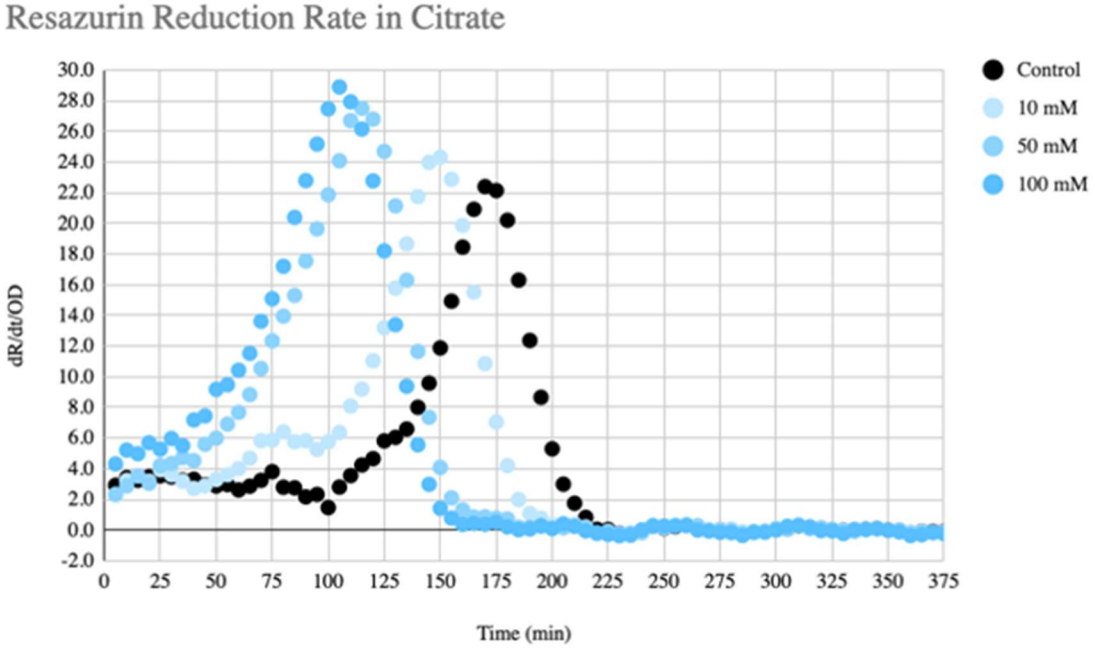

Figure 4.1 - Resazurin reduction rate in *E. coli* MG1655 exposed to citrate. Resazurin reduction rates of cell populations exposed to 10-100 mM citrate, displayed by derivative fluorescence plotted on Y-axis, and time plotted on X-axis. Values in the legend correspond to citrate concentrations used.

To perform the survival assay, we selected a concentration of citrate, 20 mM, that would be representative of both metabolic acceleration and the greatest likelihood of inducing antibiotic repotentiation without being detrimental to cell growth. We selected 10 µg/mL Kan, a concentration higher than its LDL, and 0.3M NaCl as a concentration that induces cross-protection. Cells exposed to 20 mM citrate and 0.3M NaCl experienced no growth defect after 4 hrs (**Fig. 4.2**). Cells co-exposed to NaCl, citrate, and Kan did not experience resensitization to Kan, as cells sustained 91% growth over 4 hours. The may be due to the sustained presence of NaCl in the media limiting the likelihood of cellular respiration recovery, consequently perturbing the MP and the necessary voltage required for aminoglycoside killing. Future work utilizing sucrose and metabolites that generate a voltage gradient would be suitable for future aminoglycoside repotentiation assays. Additionally, utilizing citrate, or citrate with added metabolites, while adjusting concentrations of NaCl or sucrose may be useful in establishing baseline levels of likely repotentiation. The advantages of the resazurin reduction assay makes it an ideal technique to utilize for high throughput screening of compounds for repotentiating tolerant cells to antibiotics.

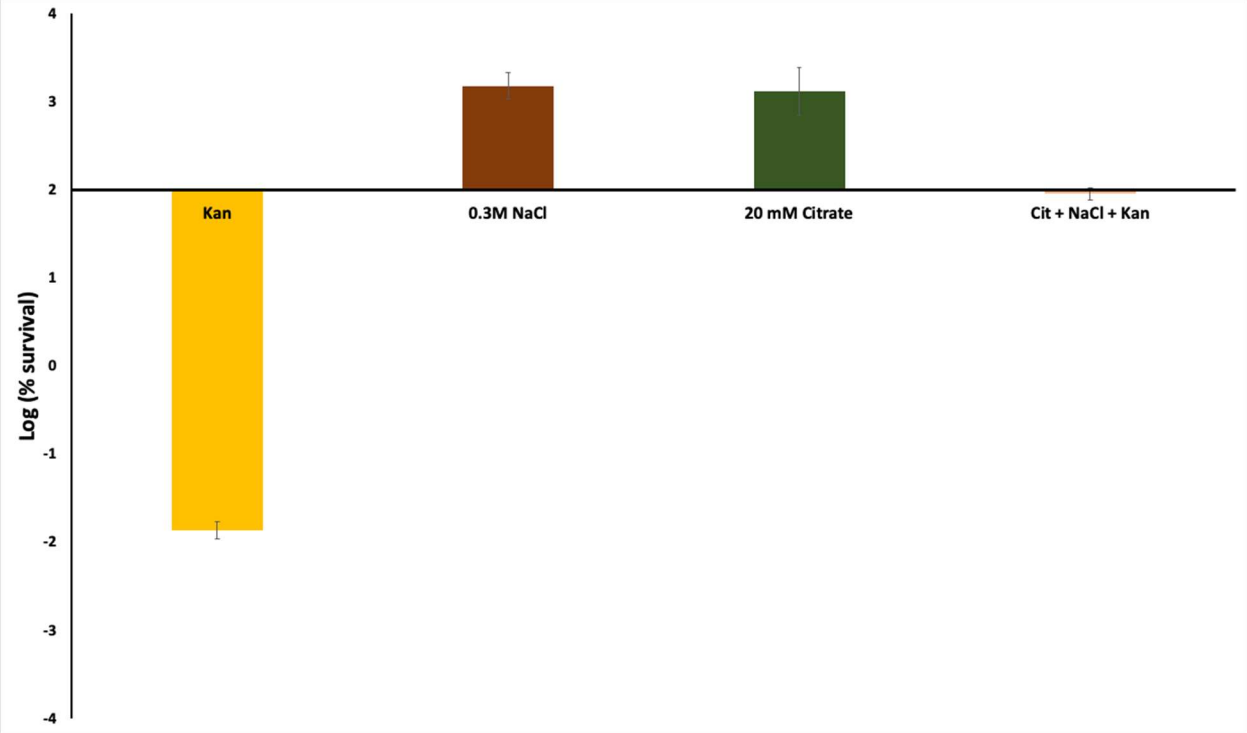

Figure 4.2 - Exposure of citrate on survival of cells treated with NaCl and Kan. The plot shows log percent survival of cells in Kan, 0.3M NaCl, 20 mM Citrate, and Citrate + NaCl (± Kan). All log percent survival values are averages of viable CFUs after 4 h exposure in 2 biological replicates and 2 technical replicates for each biological replicate in each condition. Error bars represent standard deviations.

Our future work involves, but is not limited to, resolving membrane-antibiotic interactions at high resolutions, screening the likelihood of antibiotic accumulation, and probing the activity of efflux pumps. As discussed in Ch. 3, changes in the membrane properties of cells can influence their response to antibiotics and promote tolerance. Thus, understanding the interactions between the bacterial membrane and bactericidal antibiotics is important for

understanding membrane-drug interactions for designing novel antibiotics and combating tolerance and resistance with antibiotics being used today. For this purpose, utilizing fluorescence microscopy paired with impedance spectroscopy will enable high resolution characterization of bacterial membranes. Mass spectroscopy will be used to determine the uptake of antibiotics under osmotic stress to build on the theory that uptake is not facilitated under perturbed MP conditions, especially for aminoglycosides. For β-lactams and fluoroquinolones, however, mass spectroscopy will demonstrate the effectiveness of efflux pumps in osmolyte-induced tolerance by quantifying the levels of antibiotic in the media. Furthermore, efflux pump activity will be measured via qPCR to determine if tolerance under sustained osmolyte exposure maintains the same features of antibiotic efflux as genetically manipulated models of tolerance. These assays will be used in the same manner to supplement the resazurin reduction assay in predicting antibiotic tolerance and repotentiation by way of metabolic stimulation.

[See next page for References]

[1] Nieuwlaat, R., Mbuagbaw, L., Mertz, D., Burrows, L. L., Bowdish, D., Moja, L., Wright, G. D., & Schünemann, H. J. (2021). Coronavirus Disease 2019 and Antimicrobial Resistance: Parallel and Interacting Health Emergencies. *Clinical infectious diseases : an official publication of the Infectious Diseases Society of America*, *72*(9), 1657–1659.

[2] Kariuki, S., Wairimu, C., & Mbae, C. (2021). Antimicrobial Resistance in Endemic Enteric Infections in Kenya and the Region, and Efforts Toward Addressing the Challenges. *The Journal of infectious diseases*, *224*(12 Suppl 2), S883–S889.

[3] Lishman, H., Castro-Sanchez, E., Charani, E., Mookerjee, S., Costelloe, C. (2016). The burden of antimicrobial resistant infections in black and minority ethnic groups (p. 10) [A race equality foundation briefing paper] Accessed January 9, 2022.

[4] Ham, D. C., Lutgring, J., & Sharma, A. (2019). Antimicrobial resistance - Chapter 11 - 2020 Yellow Book. Centers for Disease Control and Prevention. Accessed January 9, 2022.

[5] Centers for Disease Control and Prevention: Antibiotic Resistance Threats in the United States, 2019. Atlanta, GA: Centers for Disease Control and Prevention; Available at: https://www.cdc.gov/drugresistance/pdf/threatsreport/2019-ar-threats-report-508.pdf. Accessed January 9, 2022.

[6] Burnham, J. P., Olsen, M. A., & Kollef, M. H. (2019). Re-estimating annual deaths due to multidrug-resistant organism infections. *Infection control and hospital epidemiology*, *40*(1), 112–113.

[7] Miller, E. F., & Maier, R. J. (2014). Ammonium metabolism enzymes aid Helicobacter pylori acid resistance. *J. Bacteriol, 196*, 3074–308.

[8] Umanski, T., Rosenshine, I., & Friedberg, D. (2002). Thermoregulated expression of virulence genes in enteropathogenic Escherichia coli. *Microbiology (Reading, England)*, *148*(Pt 9), 2735–2744.

[9] Fang, F. C. (2004). Antimicrobial reactive oxygen and nitrogen species: concepts and controversies. *Nature Reviews Microbiology*, *2*(10), 820–832.

[10] Bojanovič, K., D'Arrigo, I., Long, K. S. (2017). Global Transcriptional Responses to Osmotic, Oxidative, and Imipenem Stress Conditions in Pseudomonas Putida. *Appl Environ Microbiol*, *83*(7):e03236-16.

[11] D'Costa, V. M., McGrann, K. M., Hughes, D. W., and Wright, G. D. (2006). Sampling the antibiotic resistome. *Science 311*, 374–377.

[12] Giedraitienė, A., Vitkauskienė, A., Naginienė, R., and Pavilonis, A. (2011). Antibiotic resistance mechanisms of clinically important bacteria. *Medicina,* 47:19.

[13] Cox, G., and Wright, G. D. (2013). Intrinsic antibiotic resistance: mechanisms, origins, challenges and solutions. *Int. J. Med. Microbiol, 303*, 287–292.

[14] Wiegand, I., Hilpert, K., & Hancock, R. E. (2008). Agar and broth dilution methods to determine the minimal inhibitory concentration (MIC) of antimicrobial substances. *Nature protocols*, *3*(2), 163–175.

[15] Wood, T. K., Knabel, S. J., Kwan, B. W. (2013). Bacterial persister cell formation and dormancy. *Appl Environ Microbiol, 79*:7116–7121.

[16] Windels, E. M., Michiels, J. E., Fauvart, M., Wenseleers, T., Van den Bergh, B., Michiels, J. (2019). Bacterial persistence promotes the evolution of antibiotic resistance by increasing survival and mutation rates. ISME J 13:1239–1251.

[17] Brauner, A., Fridman, O., Gefen, O., and Balaban, N. Q. (2016). Distinguishing between resistance, tolerance and persistence to antibiotic treatment. *Nat. Rev. Microbiol, 14*, 320–330.

[18] Balaban, N. Q., Helaine, S., Lewis, K., Ackermann, M., Aldridge, B., Andersson, D. I., et al. (2019). Definitions and guidelines for research on antibiotic persistence. *Nat. Rev. Microbiol, 17*, 441–448.

[19] Fridman, O., Goldberg, A., Ronin, I., Shoresh, N., and Balaban, N. Q. (2014). Optimization of lag time underlies antibiotic tolerance in evolved bacterial populations. *Nature, 513*, 418–421.

[20] Van den Bergh, B., Michiels, J. E., Wenseleers, T., Windels, E. M., Boer, P. V., Kestemont, D., et al. (2016). Frequency of antibiotic application drives rapid evolutionary adaptation of *Escherichia coli* persistence. *Nat. Microbiol, 1*, 1–7.

[21] Keren, I., Kaldalu, N., Spoering, A., Wang, Y., and Lewis, K. (2004). Persister cells and tolerance to antimicrobials. *FEMS Microbiol. Lett, 230*, 13–18.

[22] Lewis, K. (2007). Persister cells, dormancy and infectious disease. *Nat. Rev. Microbiol, 5*, 48–56.

[23] Lewis, K. (2010). Persister cells. *Annu. Rev. Microbiol, 64*, 357–372.

[24] Byrd, B. A., Zenick, B., Rocha-Granados, M. C., Englander, H. E., Hare, P. J., LaGree, T. J., DeMarco, A. M., & Mok, W. (2021). The AcrAB-TolC Efflux Pump Impacts Persistence and Resistance Development in Stationary-Phase Escherichia coli following Delafloxacin Treatment. *Antimicrobial agents and chemotherapy*, *65*(8), e0028121.

[25] Lopatkin, A. J., Bening, S. C., Manson, A. L., Stokes, J. M., Kohanski, M. A., Badran, A. H., Earl, A. M., Cheney, N. J., Yang, J. H., & Collins, J. J. (2021). Clinically relevant mutations in core metabolic genes confer antibiotic resistance. *Science (New York, N.Y.)*, *371*(6531).

[26] Pandey, S., Sahukhal, G. S., & Elasri, M. O. (2021). The *msaABCR* Operon Regulates Persister Formation by Modulating Energy Metabolism in *Staphylococcus aureus*. *Frontiers in microbiology*, *12*, 657753.

[27] Wu, N., He, L., Cui, P., Wang, W., Yuan, Y., Liu, S., Xu, T., Zhang, S., Wu, J., Zhang, W., & Zhang, Y. (2015). Ranking of persister genes in the same Escherichia coli genetic background demonstrates varying importance of individual persister genes in tolerance to different antibiotics. *Frontiers in microbiology*, *6*, 1003.

[28] Ma, C., Sim, S., Shi, W., Du, L., Xing, D., & Zhang, Y. (2010). Energy production genes sucB and ubiF are involved in persister survival and tolerance to multiple antibiotics and stresses in Escherichia coli. *FEMS microbiology letters*, *303*(1), 33–40.

[29] Wang, Y., Bojer, M. S., George, S. E., Wang, Z., Jensen, P. R., Wolz, C., Ingmer, H. (2018). Inactivation of TCA cycle enhances Staphylococcus aureus persister cell formation in stationary phase. *Sci Rep, 8*:10849.

[30] Hommes, N. G., Kurth, E. G., Sayavedra-Soto, L. A., & Arp, D. J. (2006). Disruption of sucA, which encodes the E1 subunit of alpha-ketoglutarate dehydrogenase, affects the survival of Nitrosomonas europaea in stationary phase. *Journal of bacteriology*, *188*(1), 343–347.

[31] Cesar, S., Anjur-Dietrich, M., Yu, B., Li, E., Rojas, E., Neff, N., Cooper, T. F., & Huang, K. C. (2020). Bacterial Evolution in High-Osmolarity Environments. *mBio*, *11*(4), e01191-20.

[32] Tamer, Y. T., Gaszek, I., Rodrigues, M., Coskun, F. S., Farid, M., Koh, A. Y., Russ, W., & Toprak, E. (2021). The Antibiotic Efflux Protein TolC Is a Highly Evolvable Target under Colicin E1 or TLS Phage Selection. *Molecular biology and evolution*, *38*(10), 4493–4504.

[33] Wan, Y., Wang, M., Chan, E., & Chen, S. (2021). Membrane Transporters of the Major Facilitator Superfamily Are Essential for Long-Term Maintenance of Phenotypic Tolerance to Multiple Antibiotics in E. coli. *Microbiology spectrum*, *9*(3), e0184621.

[34] Wang, M., Chan, E., Wan, Y., Wong, M. H., & Chen, S. (2021). Active maintenance of proton motive force mediates starvation-induced bacterial antibiotic tolerance in Escherichia coli. *Communications biology*, *4*(1), 1068.

[35] Zhu, M., & Dai, X. (2018). High Salt Cross-Protects *Escherichia coli* from Antibiotic Treatment through Increasing Efflux Pump Expression. *mSphere*, *3*(2), e00095-18.

[36] Jacobsen, S. M., Stickler, D. J., Mobley, H. L., & Shirtliff, M. E. (2008). Complicated catheter-associated urinary tract infections due to Escherichia coli and Proteus mirabilis. *Clinical Microbiology Reviews*, *21*(1), 26–59.

[37] Flores-Mireles, A. L., Walker, J. N., Caparon, M., & Hultgren, S. J. (2015). Urinary tract infections: epidemiology, mechanisms of infection and treatment options. *Nature Reviews Microbiology*, *13*(5), 269–284.

[38] Aberg, A., Shingler, V., & Balsalobre, C. (2006). (p)ppGpp regulates type 1 fimbriation of Escherichia coli by modulating the expression of the site-specific recombinase FimB. *Molecular microbiology*, *60*(6), 1520–1533.

[39] Alteri, C. J., & Mobley, H. (2015). Metabolism and Fitness of Urinary Tract Pathogens. *Microbiology spectrum*, *3*(3), 10.1128/microbiolspec.MBP-0016-2015.

[40] Loh, J. T., Torres, V. J., & Cover, T. L. (2007). Regulation of Helicobacter pylori cagA expression in response to salt. *Cancer research*, *67*(10), 4709–4715.

[41] Ishikawa, T., Sabharwal, D., Bröms, J., Milton, D. L., Sjöstedt, A., Uhlin, B. E., & Wai, S. N. (2012). Pathoadaptive conditional regulation of the type VI secretion system in Vibrio cholerae O1 strains. *Infection and immunity*, *80*(2), 575–584.

[42] Sévin, D. C., Stählin, J. N., Pollak, G. R., Kuehne, A., & Sauer, U. (2016). Global Metabolic Responses to Salt Stress in Fifteen Species. *PloS one*, *11*(2), e0148888.

[43] Silhavy, T. J., Kahne, D., & Walker, S. (2010). The bacterial cell envelope. *Cold Spring Harbor perspectives in biology*, *2*(5), a000414.

[44] Laimins, L. A., Rhoads, D. B., & Epstein, W. (1981). Osmotic control of kdp operon expression in Escherichia coli. *Proceedings of the National Academy of Sciences of the United States of America*, *78*(1), 464–468.

[45] Whatmore, A. M., & Reed, R. H. (1990). Determination of turgor pressure in Bacillus subtilis: a possible role for K+ in turgor regulation. *Journal of general microbiology*, *136*(12), 2521–2526.

[46] Miller, K.J., Zelt, S.C. & Bae, JH. (1991). Glycine betaine and proline are the principal compatible solutes of *Staphylococcus aureus* . *Current Microbiology 23***,** 131–137.

[47] Godard, T., Zühlke, D., Richter, G., Wall, M., Rohde, M., Riedel, K., Poblete-Castro, I., Krull, R., & Biedendieck, R. (2020). Metabolic Rearrangements Causing Elevated Proline and Polyhydroxybutyrate Accumulation During the Osmotic Adaptation Response of Bacillus Megaterium. *Frontiers in bioengineering and biotechnology*, *8*, 47.

[48] Metris, A., George, S. M., Mulholland, F., Carter, A. T., & Baranyi, J. (2014). Metabolic shift of Escherichia coli under salt stress in the presence of glycine betaine. *Applied and environmental microbiology*, *80*(15), 4745–4756.

[49] Li, F., Xiong, X. S., Yang, Y. Y., Wang, J. J., Wang, M. M., Tang, J. W., Liu, Q. H., Wang, L., & Gu, B. (2021). Effects of NaCl Concentrations on Growth Patterns, Phenotypes Associated With Virulence, and Energy Metabolism in *Escherichia coli* BW25113. *Frontiers in microbiology*, *12*, 705326.

[50] Rojas, E., Theriot, J. A., Huang, K. C., (2014). Response of *Escherichia coli* growth rate to osmotic shock. *Proc Natl Acad Sci U S A, 111*:7807–7812.

[51] Romantsov, T., Guan, Z., & Wood, J. M. (2009). Cardiolipin and the osmotic stress responses of bacteria. *Biochimica et biophysica acta*, *1788*(10), 2092–2100.

[52] Cronan, J. E. (2003). Bacterial membrane lipids: where do we stand?. *Annual review of microbiology*, *57*, 203–224.

[53] Cronan, J. E., & Vagelos, P. R. (1972). Metabolism and function of the membrane phospholipids of Escherichia coli. *Biochimica et biophysica acta*, *265*(1), 25–60.

[54] Lobritz, M. A., Belenky, P., Porter, C. B., Gutierrez, A., Yang, J. H., Schwarz, E. G., Dwyer, D. J., Khalil, A. S., & Collins, J. J. (2015). Antibiotic efficacy is linked to bacterial cellular respiration. *Proceedings of the National Academy of Sciences of the United States of America*, *112*(27), 8173–8180.

[55] Zalis, E. A., Nuxoll, A. S., Manuse, S., Clair, G., Radlinski, L. C., Conlon, B. P., Adkins, J., & Lewis, K. (2019). Stochastic Variation in Expression of the Tricarboxylic Acid Cycle Produces Persister Cells. *mBio*, *10*(5), e01930-19.

[56] Levin-Reisman, I., Ronin, I., Gefen, O., Braniss, I., Shoresh, N., & Balaban, N. Q. (2017). Antibiotic tolerance facilitates the evolution of resistance. *Science (New York, N.Y.)*, *355*(6327), 826–830.

[57] Sulaiman, J. E., & Lam, H. (2021). Evolution of Bacterial Tolerance Under Antibiotic Treatment and Its Implications on the Development of Resistance. *Frontiers in microbiology*, *12*, 617412.

[58] Liu, J., Gefen, O., Ronin, I., Bar-Meir, M., & Balaban, N. Q. (2020). Effect of tolerance on the evolution of antibiotic resistance under drug combinations. *Science (New York, N.Y.)*, *367*(6474), 200–204.

[59] Santi, I., Manfredi, P., Maffei, E., Egli, A., & Jenal, U. (2021). Evolution of Antibiotic Tolerance Shapes Resistance Development in Chronic Pseudomonas aeruginosa Infections. *mBio*, *12*(1), e03482-20.

[60] Swi ̨eciło, A., Zych-Wezyk, I. (2013). Bacterial stress response as an adaptation to life in a soil environment. *Pol. J. Environ, 22*, 1577–1587.

[61] Giuliodori, A. M., Gualerzi, C. O., Soto, S., Vila, J., Tavio, M. M., (2007) Review on bacterial stress topics. *Ann. N. Y. Acad, 1113*, 95–104.

[62] Flores-Kim, J., Darwin, A.J. (2014). Regulation of bacterial virulence gene expression by cell envelope stress responses. *Virulence, 5*, 835–851.

[63] Begley, M., Gahan, C. G., & Hill, C. (2002). Bile stress response in Listeria monocytogenes LO28: adaptation, cross-protection, and identification of genetic loci involved in bile resistance. *Applied and environmental microbiology*, *68*(12), 6005–6012.

[64] Goodson, M., and Rowbury, R. (1989). Habituation to normally lethal acidity by prior growth of *Escherichia coli* at a sub-lethal acid pH value. *Letters in Applied Microbiology, 8*, 77-79.

[65] Al-Nabulsi, A. A., Osaili, T. M., Shaker, R. R., Olaimat, A. N., Jaradat, Z. W., Zain Elabedeen, N. A., & Holley, R. A. (2015). Effects of osmotic pressure, acid, or cold stresses on antibiotic susceptibility of Listeria monocytogenes. *Food microbiology*, *46*, 154–160.

[66] Battesti, A., Majdalani, N., & Gottesman, S. (2011). The RpoS-mediated general stress response in Escherichia coli. *Annual review of microbiology*, *65*, 189–213.

[67] Jenkins, D. E., Schultz, J. E., & Matin, A. (1988). Starvation-induced cross protection against heat or H2O2 challenge in Escherichia coli. *Journal of bacteriology*, *170*(9), 3910–3914.

[68] Leyer, G. J., & Johnson, E. A. (1993). Acid adaptation induces cross-protection against environmental stresses in Salmonella Typhimurium. *Applied and environmental microbiology*, *59*(6), 1842–1847.

[69] Wang, G., & Doyle, M. P. (1998). Heat shock response enhances acid tolerance of Escherichia coli O157:H7. *Letters in applied microbiology*, *26*(1), 31–34.

[70] Nguyen, D., Joshi-Datar, A., Lepine, F., Bauerle, E., Olakanmi, O., Beer, K., McKay, G., Siehnel, R., Schafhauser, J., Wang, Y., et al. (2011) Active starvation responses mediate antibiotic tolerance in biofilms and nutrient-limited bacteria. *Science, 334*, 982–986.

[71] Lewis, K. (2007). Persister cells, dormancy and infectious disease. *Nat. Rev. Microbiol, 5,* 48–56.

[72] Sharma, D., Misba, L., Khan, A.U. (2019). Antibiotics versus biofilm: An emerging battleground in microbial communities. *Antimicrob Resist. Infect. Control, 8*, 76.

[73] Sheikh, S.W., Ali, A., Ahsan, A., Shakoor, S., Shang, F., Xue, T. (2021). Insights into emergence of antibiotic resistance in acid-adapted enterohaemorrhagic Escherichia coli. *Antibiotics, 10*, 522.

[74] Mitosch, K., Rieckh, G., & Bollenbach, T. (2017). Noisy Response to Antibiotic Stress Predicts Subsequent Single-Cell Survival in an Acidic Environment. *Cell systems*, *4*(4), 393–403.e5.

[75] Yurtsev, E. A., Conwill, A., & Gore, J. (2016). Oscillatory dynamics in a bacterial cross-protection mutualism. *Proc. Natl Acad. Sci. USA*, 6236–6241.

[76] McMahon, M. A., Xu, J., Moore, J. E., Blair, I. S., & McDowell, D. A. (2007). Environmental stress and antibiotic resistance in food-related pathogens. *Applied and environmental microbiology*, *73*(1), 211–217.

[77] Allison, K. R., Brynildsen, M. P., & Collins, J. J. (2011). Metabolite-enabled eradication of bacterial persisters by aminoglycosides. *Nature*, *473*(7346), 216–220.

[78] Lu, T. K., & Collins, J. J. (2009). Engineered bacteriophage targeting gene networks as adjuvants for antibiotic therapy. *Proceedings of the National Academy of Sciences of the United States of America*, *106*(12), 4629–4634.

[79] Walker, S. A., McGeer, A. E., Simor, M., Armstrong-Evans, M., & Loeb, M. (2000). Why are antibiotics prescribed for asymptomatic bacteriuria in institutionalized elderly people? A qualitative study of physicians' and nurses' perceptions. *Can. Med. Assoc. J, 163*, 273-277.

[80] Cravens, D. D., & Zweig, S. (2000). Urinary catheter management. *Am. Fam. Physician 61*, 369-376.

[81] Graf, A. C. et al., (2019). Virulence Factors Produced by Staphylococcus aureus Biofilms Have a Moonlighting Function Contributing to Biofilm Integrity Authors Virulence Factors Produced by Staphylococcus aureus Biofilms Have a Moonlighting Function Contributing to Biofilm Integrity. *Mol. Cell. Proteomics, 18,* 1036–1053.

[82] Romling, U., & Balsalobre, C. (2012). Biofilm infections, their resilience to therapy and innovative treatment strategies. *J. Intern. Med, 272*, 541–561.

[83] Yaakop, A., Chan, K. G., Ee, R. *et al.* (2016). Characterization of the mechanism of prolonged adaptation to osmotic stress of *Jeotgalibacillus malaysiensis* via genome and transcriptome sequencing analyses. *Sci Rep 6*, 33660.

[84] Saba Ranjbar, "Chapter 5: *Escherichia coli* Induces Cross-protection Tolerance to Antibiotic through Osmotic Stress," PhD diss., (University of California, Irvine, 2020).

[85] Lee, J. W., Choi, S., Park, J. H., Vickers, C. E., Nielsen, L. K., & Lee, S. Y., (2010). Development of sucroseutilizing Escherichia coli K-12 strain by cloning β -fructofuranosidases and its application for Lthreonine production. *Appl. Microbiol. Biotechnol*, *88*, 905–913.

[86] Mohamed, E.T., Mundhada, H., Landberg, J. *et al.* (2019). Generation of an *E. coli* platform strain for improved sucrose utilization using adaptive laboratory evolution. *Microb Cell Fact 18,* 116.

[87] Brauner, A., Shoresh, N., Fridman, O., Balaban, N. Q. (2017). An Experimental Framework for Quantifying Bacterial Tolerance. *Biophys J, 112*(12):2664-2671.

[88] Yoshikawa, T. T., Nicolle, L. E., & Norman, D. C. (1996). Management of complicated urinary tract infection in older patients. *J. Am. Geriatr. Soc, 44*, 1235-1241.

[89] Tang, Y. H., Lu, P. L., Huang, H. Y., & Lin, Y. C. (2022). Clinical effectiveness of beta-lactams versus fluoroquinolones as empirical therapy in patients with diabetes mellitus hospitalized for urinary tract infections: A retrospective cohort study. *PloS one*, *17*(3), e0266416.

[90] Shabala, L., Bowman, J., Brown, J., Ross, T., McMeekin, T., & Shabala, S. (2009). Ion transport and osmotic adjustment in Escherichia coli in response to ionic and non-ionic osmotica. *Environmental microbiology*, *11*(1), 137–148.

[91] Choi, U., & Lee, C. R. (2019). Distinct Roles of Outer Membrane Porins in Antibiotic Resistance and Membrane Integrity in Escherichia coli. *Frontiers in microbiology*, *10*, 953.

[92] Pu, Y., Zhao, Z., Li, Y., Zou, J., Ma, Q., Zhao, Y., Ke, Y., Zhu, Y., Chen, H., Baker, M. A. B., Ge H., Sun, Y., Xie, X.S., Bai, F. (2016). Enhanced Efflux Activity Facilitates Drug Tolerance in Dormant Bacterial Cells. *Mol Cell, 62*(2), 284-294.

[93] Anes, J., McCusker, M. P., Fanning, S., & Martins, M. (2015). The ins and outs of RND efflux pumps in Escherichia coli. *Frontiers in microbiology*, *6*, 587.

[94] Shan, Y., Brown Gandt, A., Rowe, S. E., Deisinger, J. P., Conlon, B. P., & Lewis, K. (2017). ATP-Dependent Persister Formation in Escherichia coli. *mBio*, *8*(1), e02267-16.

[95] Bruni, G. N., Kralj, J. M. (2020). Membrane voltage dysregulation driven by metabolic dysfunction underlies bactericidal activity of aminoglycosides. *Elife, 9*, e58706.

[96] Soman, V., Kumari, S., Nath, S., & Elangovan, R. (2020). The Response of Bacterial Flagellar Motor to Stepwise Increase in NaCl Concentration. bioRxiv 2020.08.19.257477 [**Preprint**]. Available from: https://doi.org/10.1101/2020.08.19.257477.

[97] Greenwood, D., & O'Grady, F. (1972). The effect of osmolality on the response of Escherichia coli and Proteus mirabilis to penicillins. *British journal of experimental pathology*, *53*(5), 457–464.

[98] Lopatkin, A.J., Stokes, J.M., Zheng, E.J., Yang, J.H., Takahashi, M.K., You, L., and Collins, J.J. (2019). Bacterial metabolic state more accurately predicts antibiotic lethality than growth rate. *Nat. Microbiol, 4,* 2109–2117.

[99] Stokes, J.M., Lopatkin, A.J., Lobritz, M.A., and Collins, J.J. (2019). Bacterial metabolism and antibiotic efficacy. *Cell Metab, 30*, 251–259

[100] Gutierrez, A., Jain, S., Bhargava, P., Hamblin, M., Lobritz, M.A., and Collins, J.J. (2017). Understanding and sensitizing density-dependent persistence to quinolone antibiotics. *Mol. Cell 68*, 1147–1154

[101] Nabb, D. L., Song, S., Kluthe, K. E., Daubert, T. A., Luedtke, B. E., & Nuxoll, A. S. (2019). Polymicrobial Interactions Induce Multidrug Tolerance in *Staphylococcus aureus* Through Energy Depletion. *Frontiers in microbiology*, *10*, 2803.

[102] Amini, S., Hottes, A. K., Smith, L. E., & Tavazoie, S. (2011). Fitness landscape of antibiotic tolerance in Pseudomonas aeruginosa biofilms. *PLoS pathogens*, *7*(10), e1002298.

[103] Benarroch, J. M., & Asally, M. (2020). The Microbiologist's Guide to Membrane Potential Dynamics. *Trends in microbiology*, *28*(4), 304–314.

[104] Webster, C.M., Woody, A.M., Fusseini, S. *et al.* (2022) Proton motive force underpins respiration-mediated potentiation of aminoglycoside lethality in pathogenic *Escherichia coli*. *Arch Microbiol, 204*, 120.

[105] Farha, M. A., French, S., Stokes, J. M., & Brown, E. D. (2018). Bicarbonate alters bacterial susceptibility to antibiotics by targeting the proton motive force. *ACS Infect. Dis,* 4, 382–390.

[106] Alteri, C. J., Lindner, J. R., Reiss, D. J., Smith, S. N., & Mobley, H. L. (2011). The broadly conserved regulator PhoP links pathogen virulence and membrane potential in *Escherichia coli*. *Mol. Microbiol,* 82, 145–163.

[107] Verstraeten, N., Knapen, W. J., Kint, C. I., Liebens, V., Van den Bergh, B., Dewachter, L., Michiels, J. E., Fu, Q., David, C. C., Fierro, A. C., Marchal, K., Beirlant, J., Versées, W., Hofkens, J., Jansen, M., Fauvart, M., & Michiels, J. (2015). Obg and Membrane Depolarization Are Part of a Microbial Bet-Hedging Strategy that Leads to Antibiotic Tolerance. *Molecular cell*, *59*(1), 9–21.

[108] Zheng, E.J., Andrews, I.W., Grote, A.T. *et al.* (2022). Modulating the evolutionary trajectory of tolerance using antibiotics with different metabolic dependencies. *Nat Commun 13*, 2525.

[109] Bigalke, D. L. (1984). Methods used for monitoring the microbiological quality of raw milk. *Dairy Food Sanit, 4*, 189–190.

[110] Drummond, A. J., Waigh, R. D. (2000). The development of microbiological methods for phytochemical screening. In: Pandalai S, editor. *Recent research developments in phytochemistry.* India: Research Signpost.

[111] McNicholl, B. P., McGrath, J. W., Quinn, J. P. (2006). Development and application of a resazurin-based biomass activity test for activated sludge plant management. *Water Res, 41,* 127–133.

[112] Sarker, S.D., Nahar, L., Kumarasamy, Y. (2007). Microtitre plate-based antibacterial assay incorporating resazurin as an indicator of cell growth, and its application in the in vitro antibacterial screening of phytochemicals. *Methods, 42,* 321–324.

[113] Martin, A., Takiff, H., Vandamme, P., Swings, J., Palomino, J. C., & Portaels, F. (2006). A new rapid and simple colorimetric method to detect pyrazinamide resistance in Mycobacterium tuberculosis using nicotinamide. *The Journal of antimicrobial chemotherapy*, *58*(2), 327–331.

[114] O'Brien, J., Wilson, I., Orton, T., & Pognan, F. (2000). Investigation of the Alamar Blue (resazurin) fluorescent dye for the assessment of mammalian cell cytotoxicity. *European journal of biochemistry*, *267*(17), 5421–5426.

[115] Yixin Huang, Ongoing dissertation research in the mechanisms of resazurin reduction in *E. coli*, PhD diss., (University of California, Irvine, Date TBD).

[116] Rojas-Andrade, M., & Hochbaum, A. I. (2022). Metabolic tracking and rapid antibiotic susceptibility determination enabled by short timescale resazurin reduction dynamics. Manuscript in preparation.

[117] Damper, P. D., Epstein, W. (1981). Role of the membrane potential in bacterial resistance to aminoglycoside antibiotics. *Antimicrob Agents Chemother*, (6), 803-8.

[118] Rampersad, S.N. (2012). Multiple applications of alamar blue as an indicator of metabolic function and cellular health in cell viability bioassays. *Sensors, 12*, 12347–12360.

[119] Lee, D. D., Galera-Laporta, L., Bialecka-Fornal, M., Moon, E. C., Shen, Z., Briggs, S. P., Garcia-Ojalvo, J., & Süel, G. M. (2019). Magnesium Flux Modulates Ribosomes to Increase Bacterial Survival. *Cell*, *177*(2), 352–360.e13.

[120] Bot, C. T., Prodan, C. (2010). Quantifying the membrane potential during E. coli growth stages. *Biophys Chem, 146*(2-3), 133-7.

[121] Jin, X., Zhang, X., Ding, X., Tian, T., Tseng, C., Luo, X., Chen, X., Lo, C., Leake, M. C., & Bai, F. (2022). Sensitive bacterial Vm sensors revealed the excitability of bacterial Vm and its role in antibiotic tolerance. bioRxiv 2022.06.02.494477 **[Preprint]**. Available from: https://doi.org/10.1101/2022.06.02.494477

[122] Masi, M., Réfregiers, M., Pos, K. M., Pagès, J. M. (2017). Mechanisms of envelope permeability and antibiotic influx and efflux in Gram-negative bacteria. *Nat Microbiol, 2*, 17001.

[123] Delcour, A. H. (2009). Outer membrane permeability and antibiotic resistance. *Biochimica et biophysica acta*, *1794*(5), 808–816.

[124] Peng, B., Su, Y. B., Li, H., Han, Y., Guo, C., Tian, Y. M., & Peng, X. X. (2015). Exogenous alanine and/or glucose plus kanamycin kills antibiotic-resistant bacteria. *Cell metabolism*, *21*(2), 249–262.

[125] Su, Y. B., Peng, B., Li, H., Cheng, Z. X., Zhang, T. T., Zhu, J. X., Li, D., Li, M. Y., Ye, J. Z., Du, C. C., Zhang, S., Zhao, X. L., Yang, M. J., & Peng, X. X. (2018). Pyruvate cycle

increases aminoglycoside efficacy and provides respiratory energy in bacteria. *Proceedings of the National Academy of Sciences of the United States of America*, *115*(7), E1578–E1587.

[126] Meylan, S., Porter, C. B. M., Yang, J. H., Belenky, P., Gutierrez, A., Lobritz, M. A., Park, J., Kim, S. H., Moskowitz, S. M., & Collins, J. J. (2017). Carbon Sources Tune Antibiotic Susceptibility in Pseudomonas aeruginosa via Tricarboxylic Acid Cycle Control. *Cell chemical biology*, *24*(2), 195–206.

[127] Su, Y. B., Peng, B., Han, Y., Li, H., & Peng, X. X. (2015). Fructose restores susceptibility of multidrug-resistant Edwardsiella tarda to kanamycin. *Journal of proteome research*, *14*(3), 1612–1620.